5.2 Phyllosilicates

5. **PHYLLOSILICATES (leaf, sheet) three O are shared Si_2O_5, Si/O=2.5,**

- **Low specific density,**
- **One prominent cleavage,**
- **Contains OH group,**
- **Important part of soil clays.**

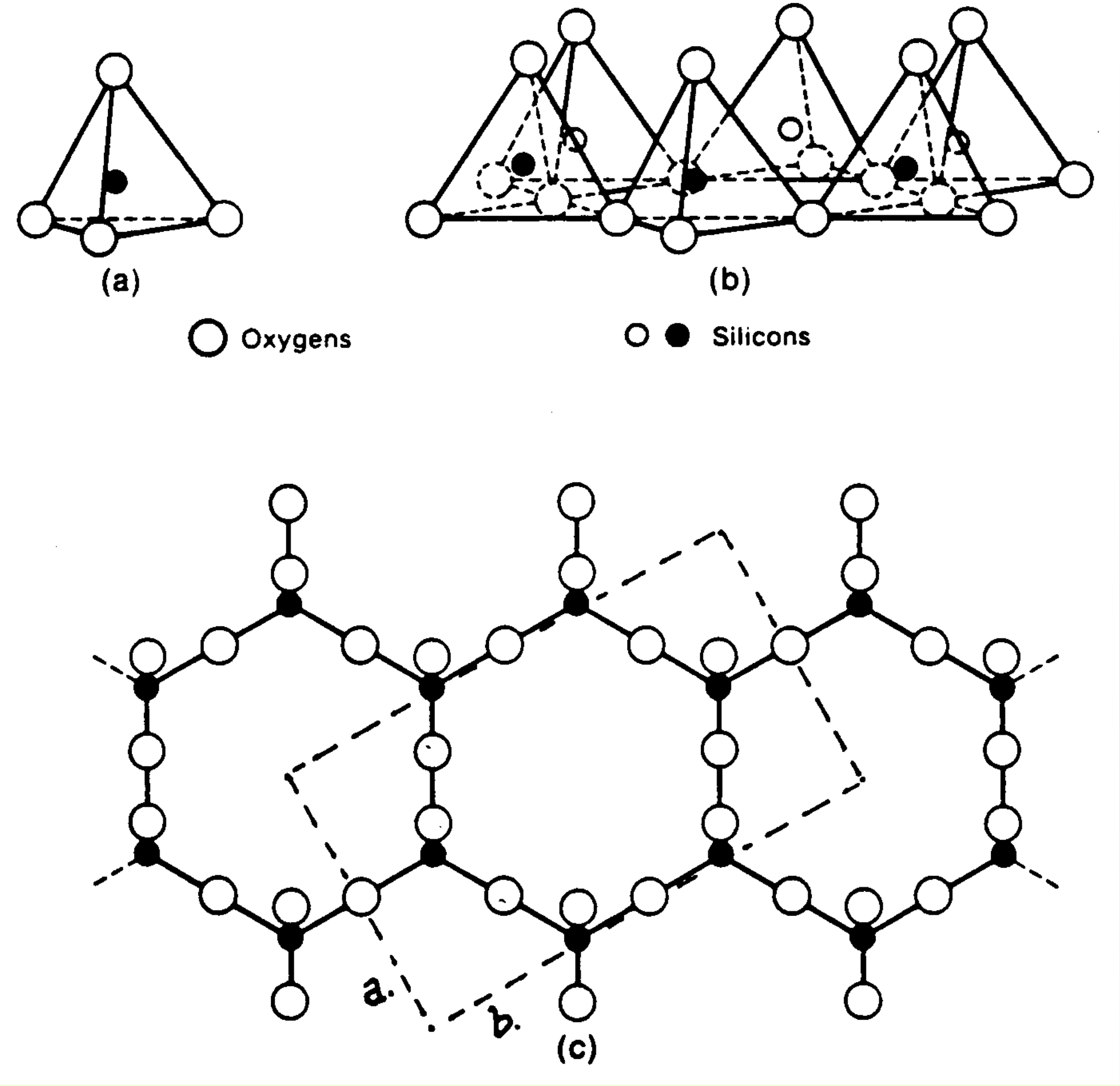

(a) single silica tetrahedron; (b) silica tetrahedron arranged in a hexagonal network; (c) three hexagons joined into double chain and extends in all directions in this plane forming a tetrahedron sheet. Silicon and apical oxygens are projected onto the plane of the base of tetrahedron.

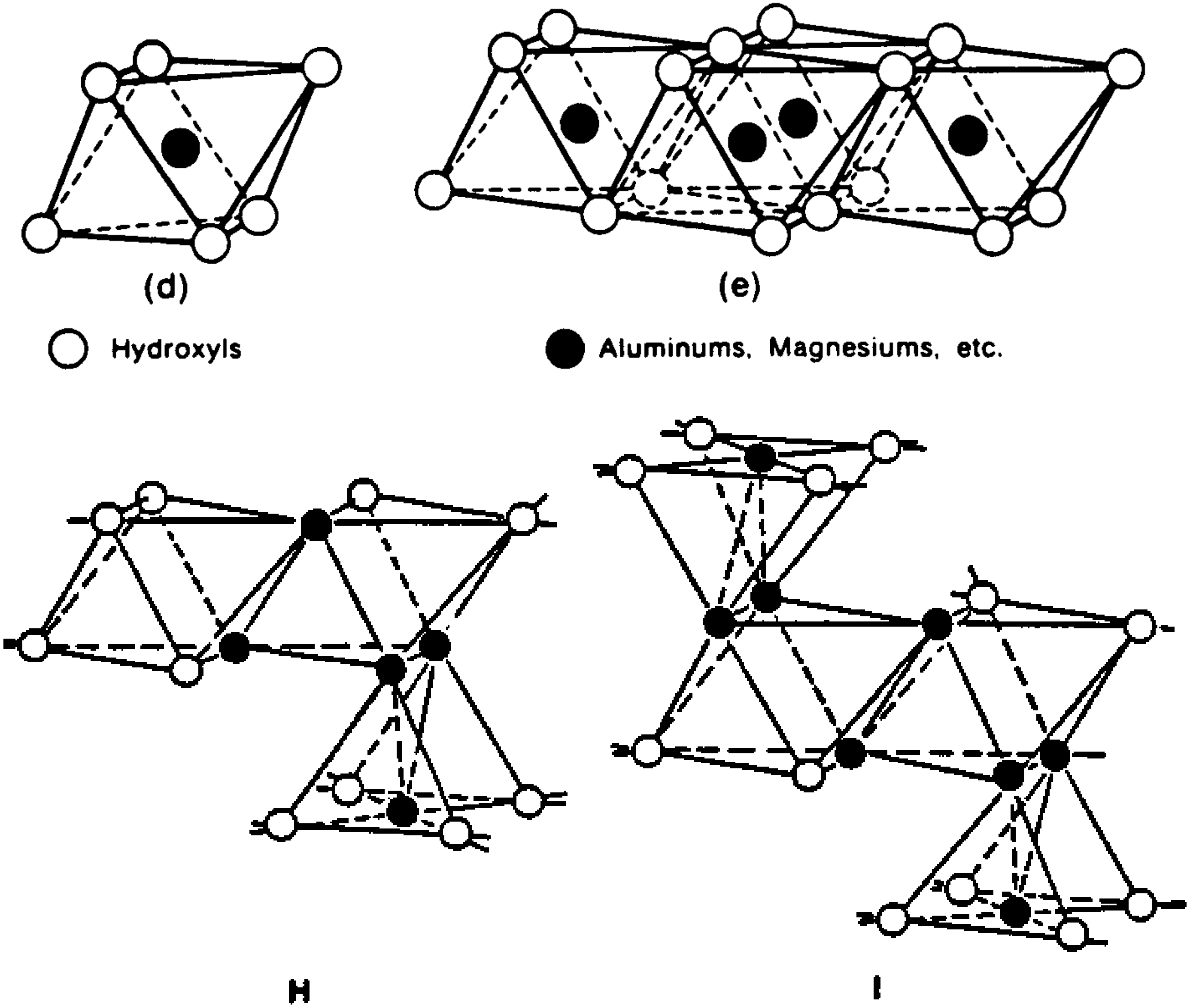

(d) A single octahedral unit; (e) Several octahedral units joined into the octahedral sheet structure, (H) and (I) combination of tetrahedron and octahedron combinations.

The atomic radii of a number of ions common in clays.

Ion	Radius Å	Found in
Si^{4+}	0.41	Silica tetrahedra (ideal fit)
Al^{3+}	0.50	Silica tetrahedra (fits tight)
Fe^{2+}	0.74	Alumina octahedra (ideal fit)
Fe^{3+}	0.64	Alumina octahedra (fits tight)
Mg^{2+}	0.65	// // // //
Ca^{2+}	0.94	Do not fit-----Only on exchange sites
Na^{+}	0.98	// // // // // // //
K^{+}	1.33	// // // // // // //

BASIC STRUCTURE OF CLAY MINERALS

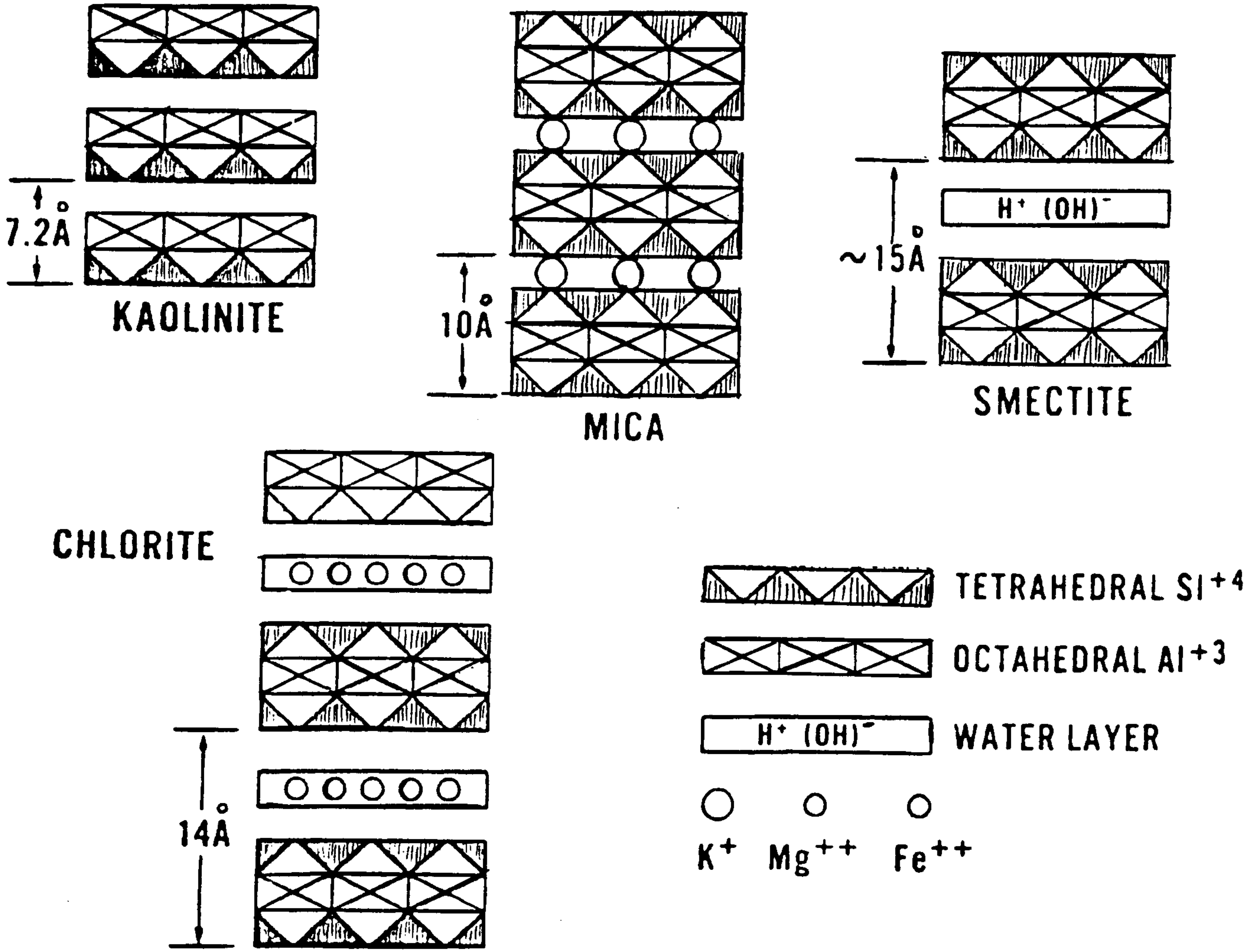

Sheets of Tetrahedron and Octahedron

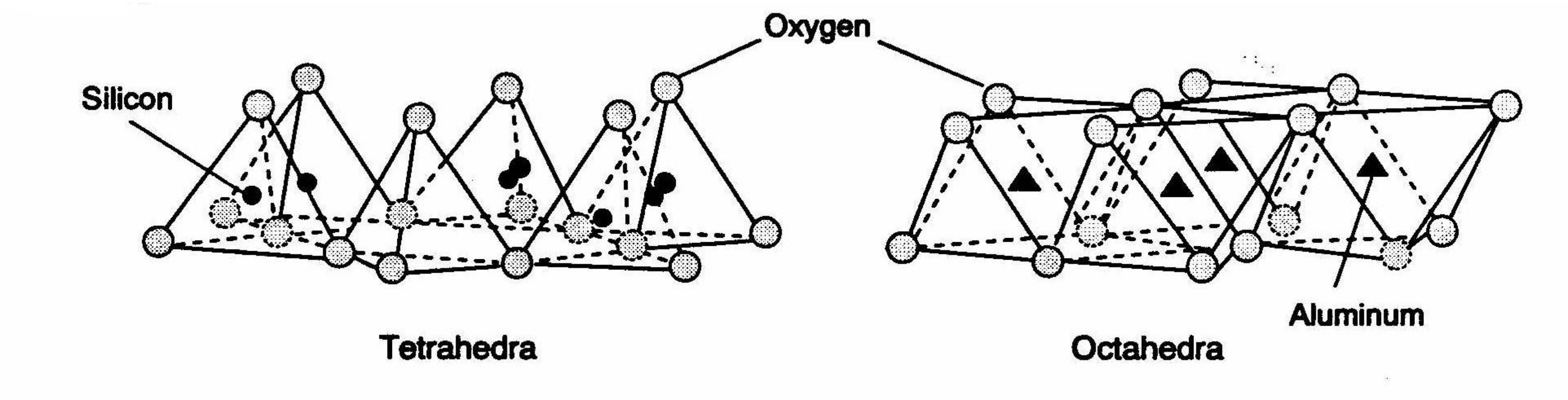

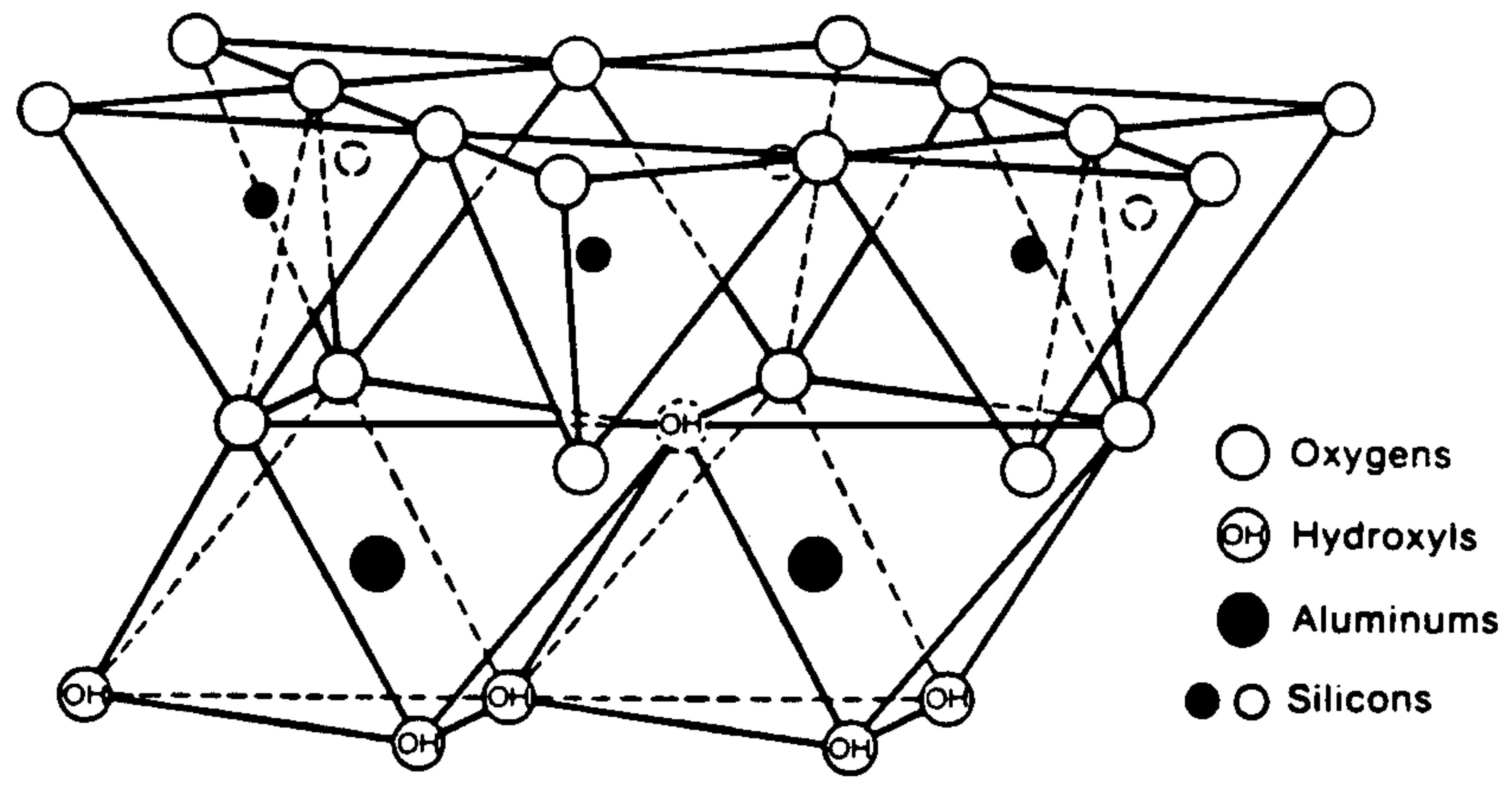

Sketch of kaolinite, 1:1 dioctahedral phyllosilicate. (From Grim, 1968, Fig. 4.4).

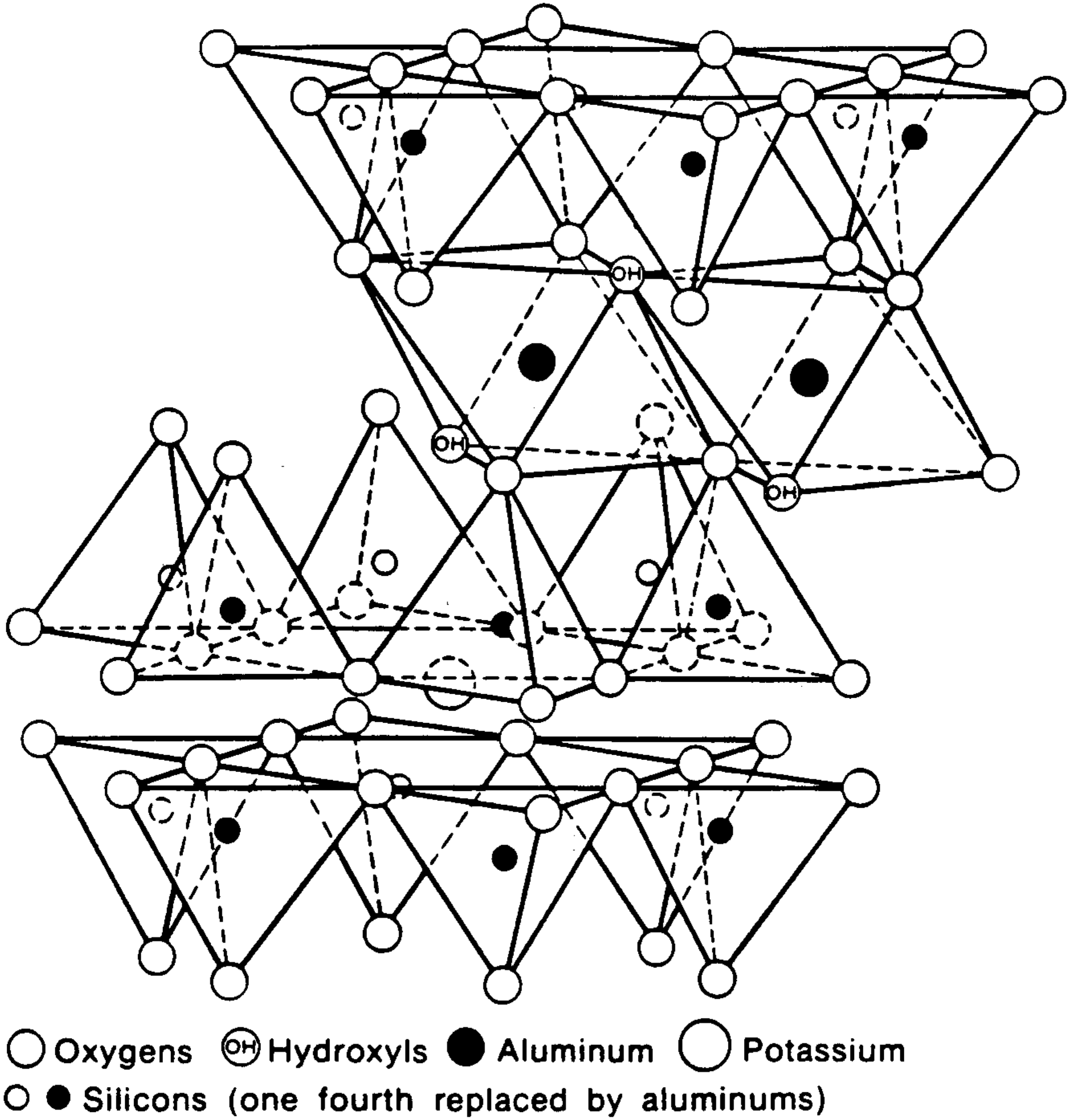

Sketch of muscovite, a 2:1 dioctahedral phyllosilicate. (From Grim 1968, Fig. 4.16).

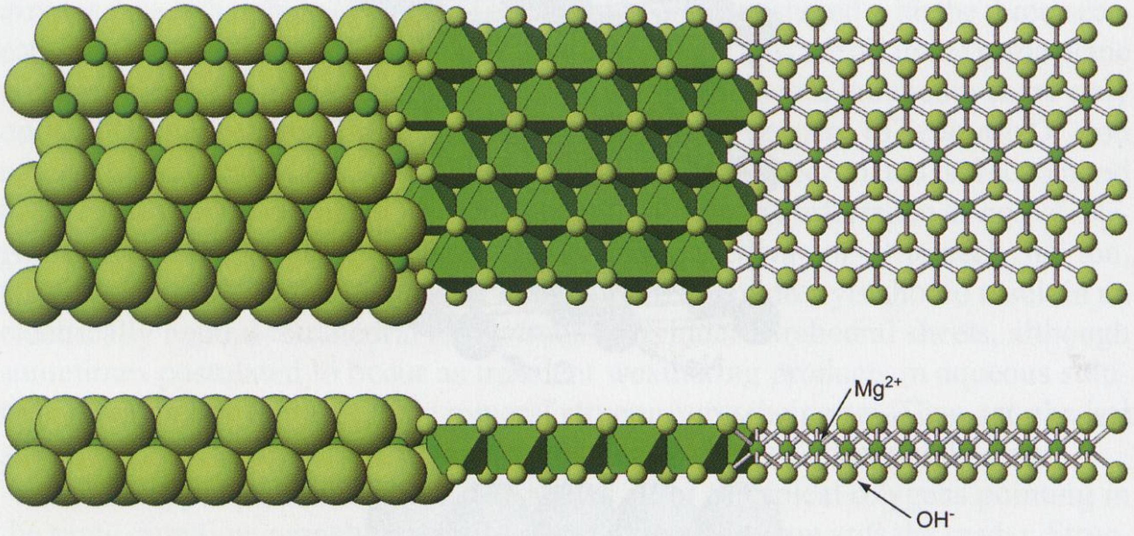

a The Octahedral Sheet (trioctahedral)

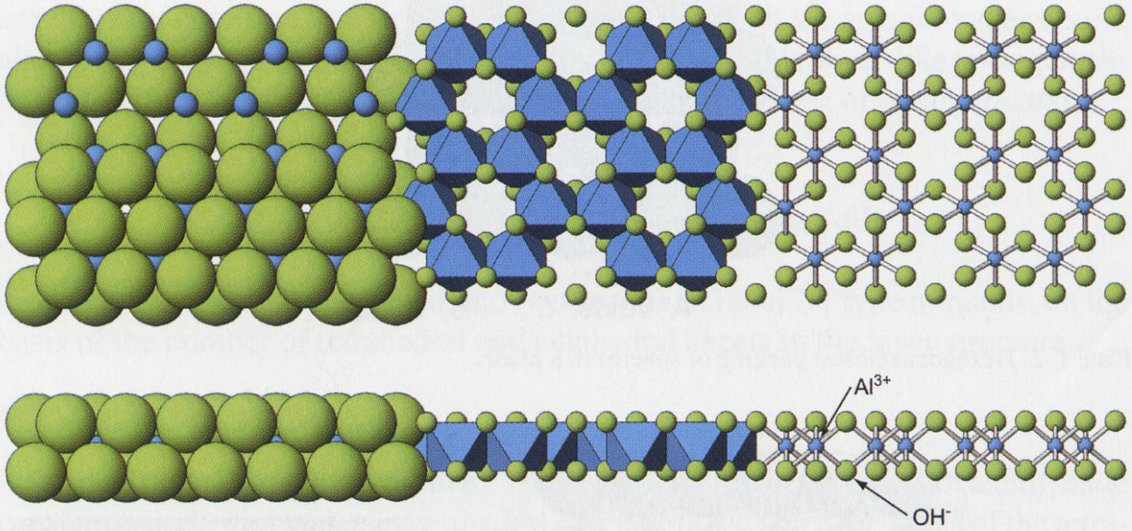

b The Octahedral Sheet (dioctahedral)

Plate 1–4. The octahedral sheet. (a) A trioctahedral sheet. (b) A dioctahedral sheet.

The Tetrahedral Sheet

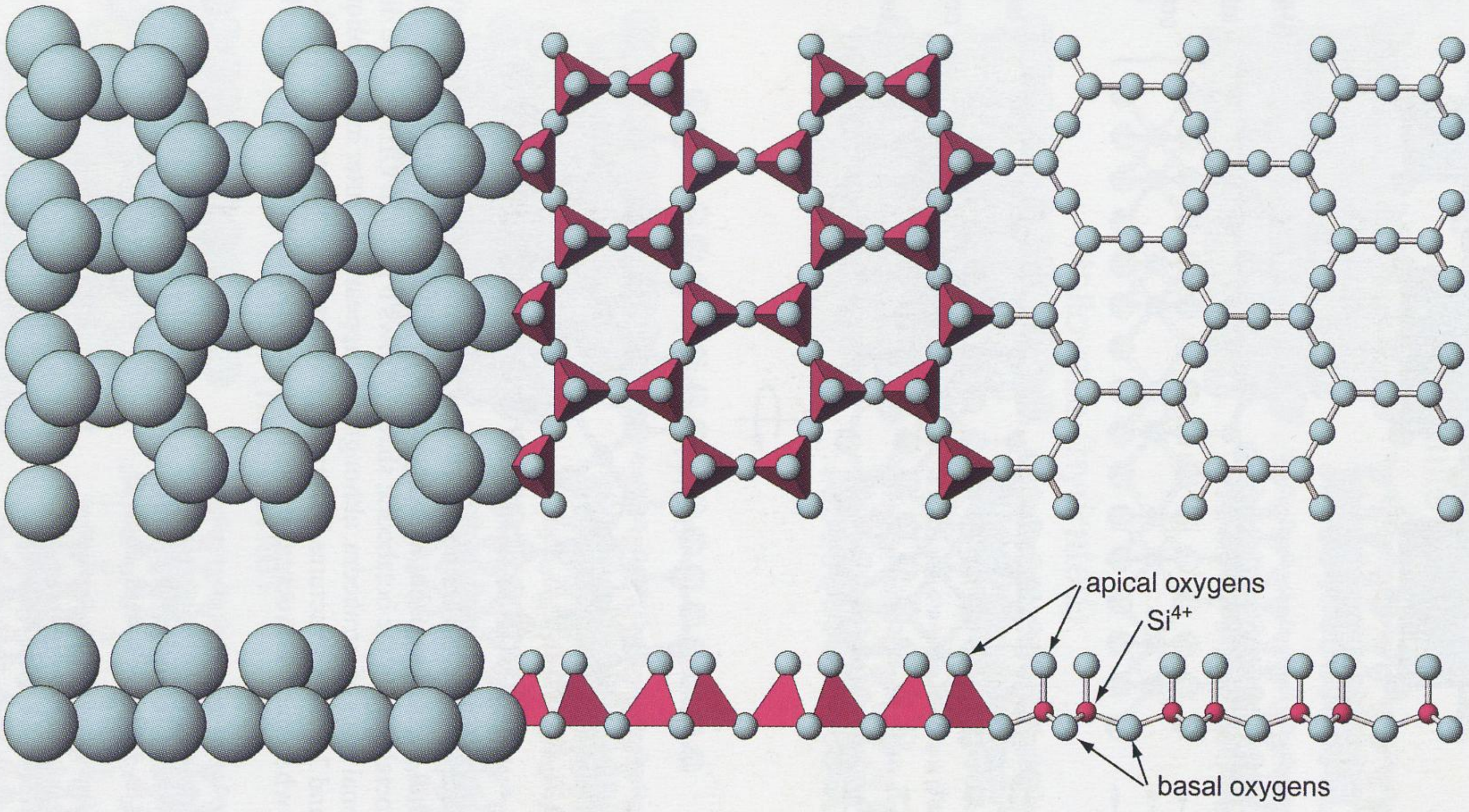

etrahedral sheet.

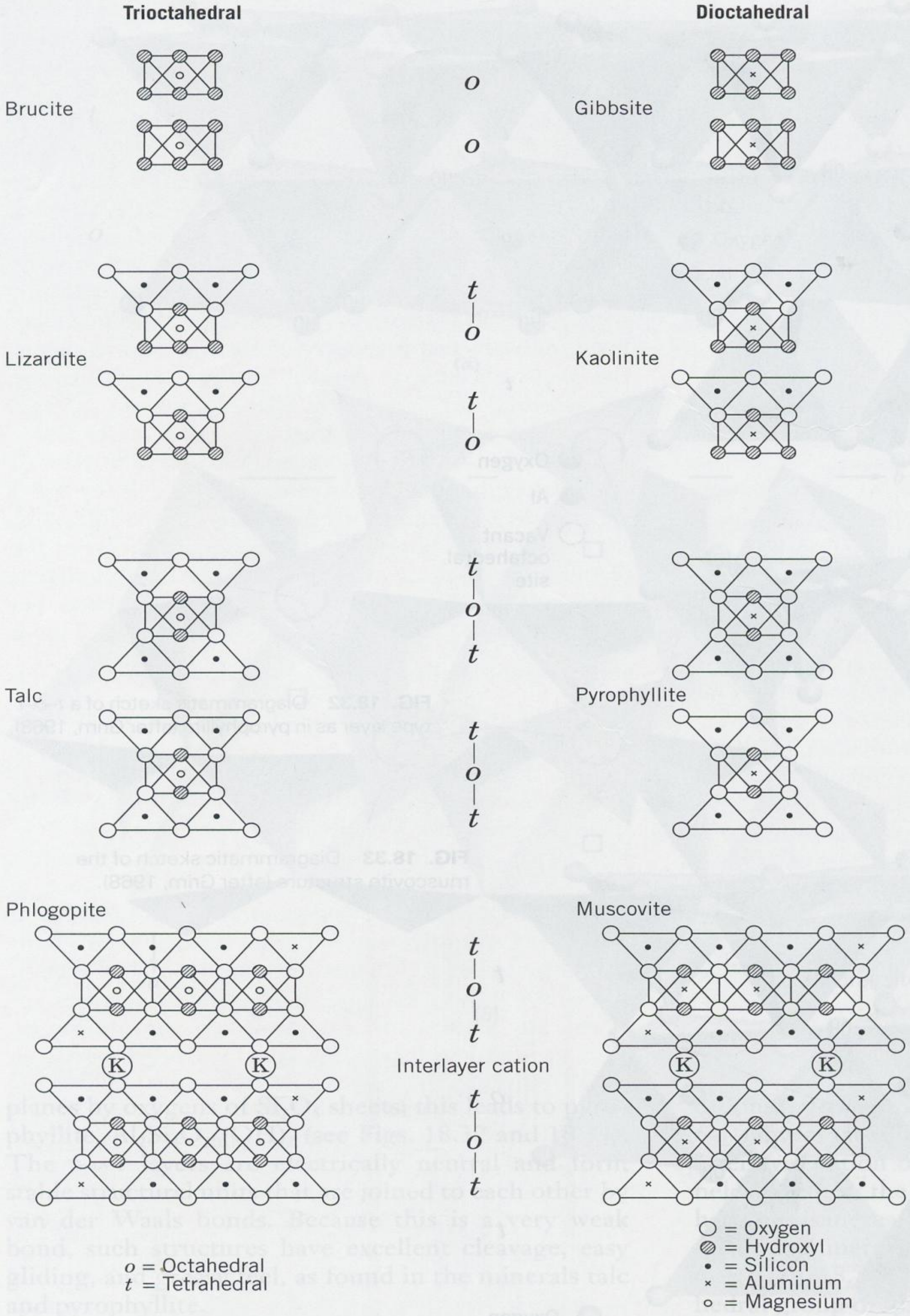
Trioctahedral
Dioctahedral
Brucite
Gibbsite
o
o
Lizardite
Kaolinite
t—o
t—o
Talc
Pyrophyllite
t—o—t
t—o—t
Phlogopite
Muscovite
t—o—t
Interlayer cation
t—o—t
K
K
K
K
o = Octahedral
t = Tetrahedral
○ = Oxygen
▨ = Hydroxyl
• = Silicon
× = Aluminum
○ = Magnesium

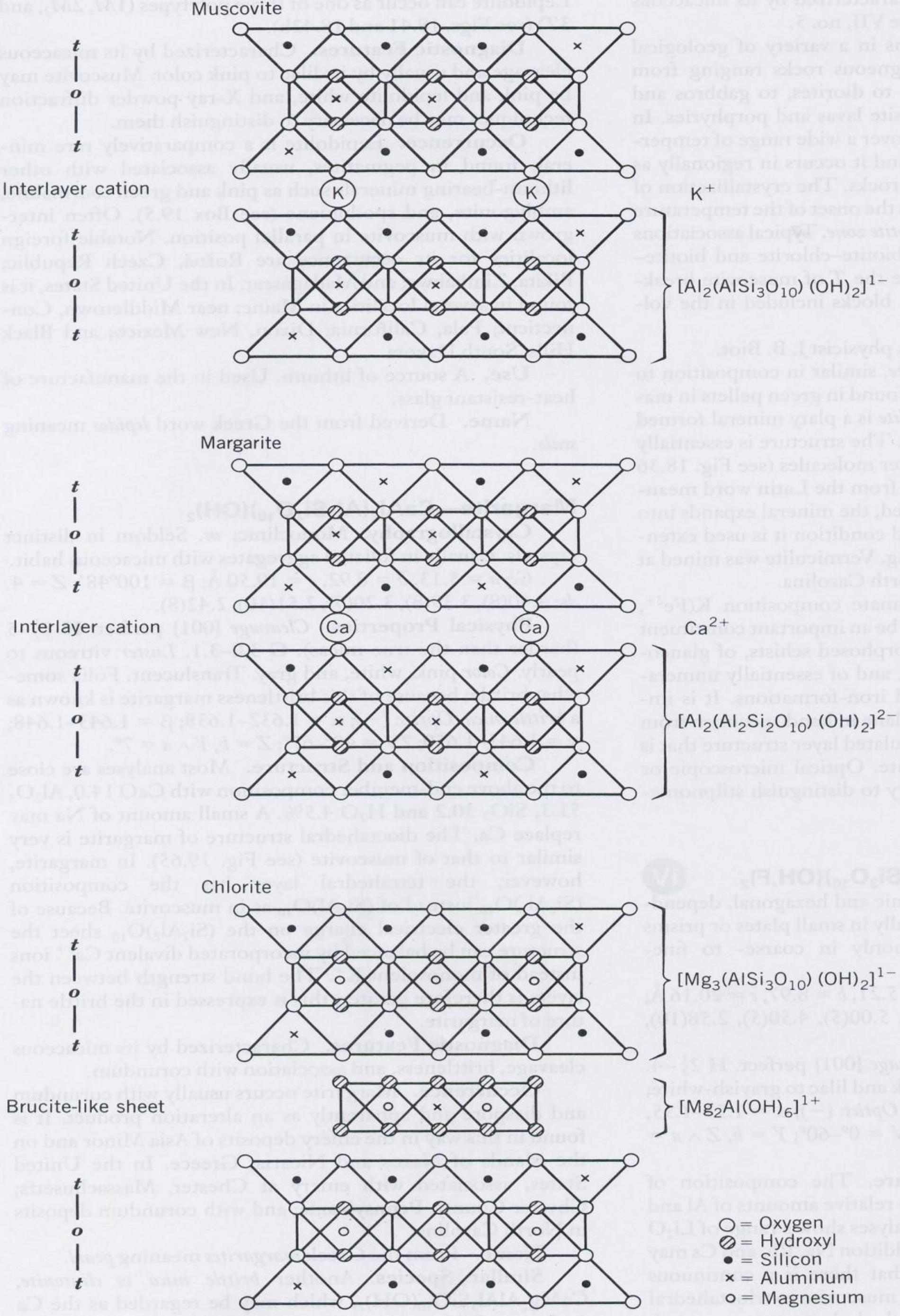

FIG. 19.65 Schematic development of the structures and compositions of muscovite, margarite, and chlorite (compare with Fig. 18.34).

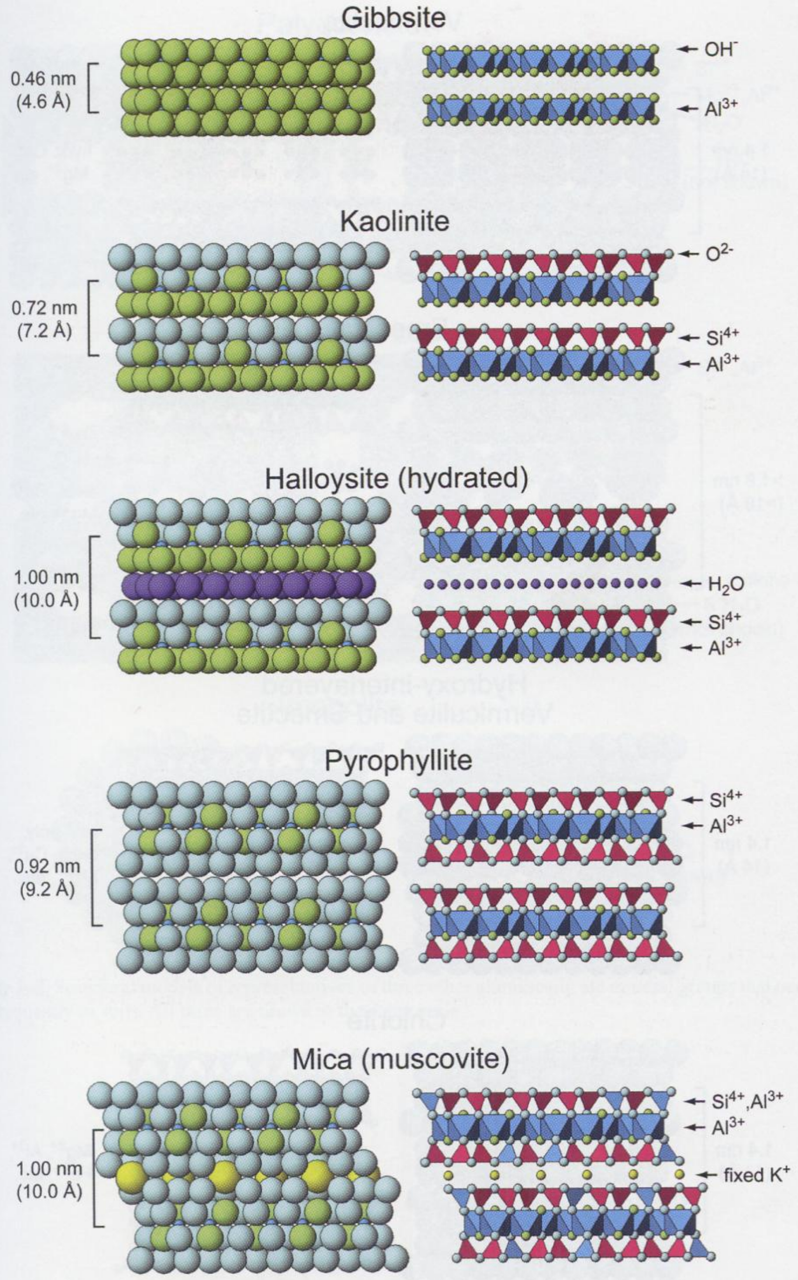

late 1–7. Structural scheme of soil minerals based on octahedral and tetrahedral sheets.

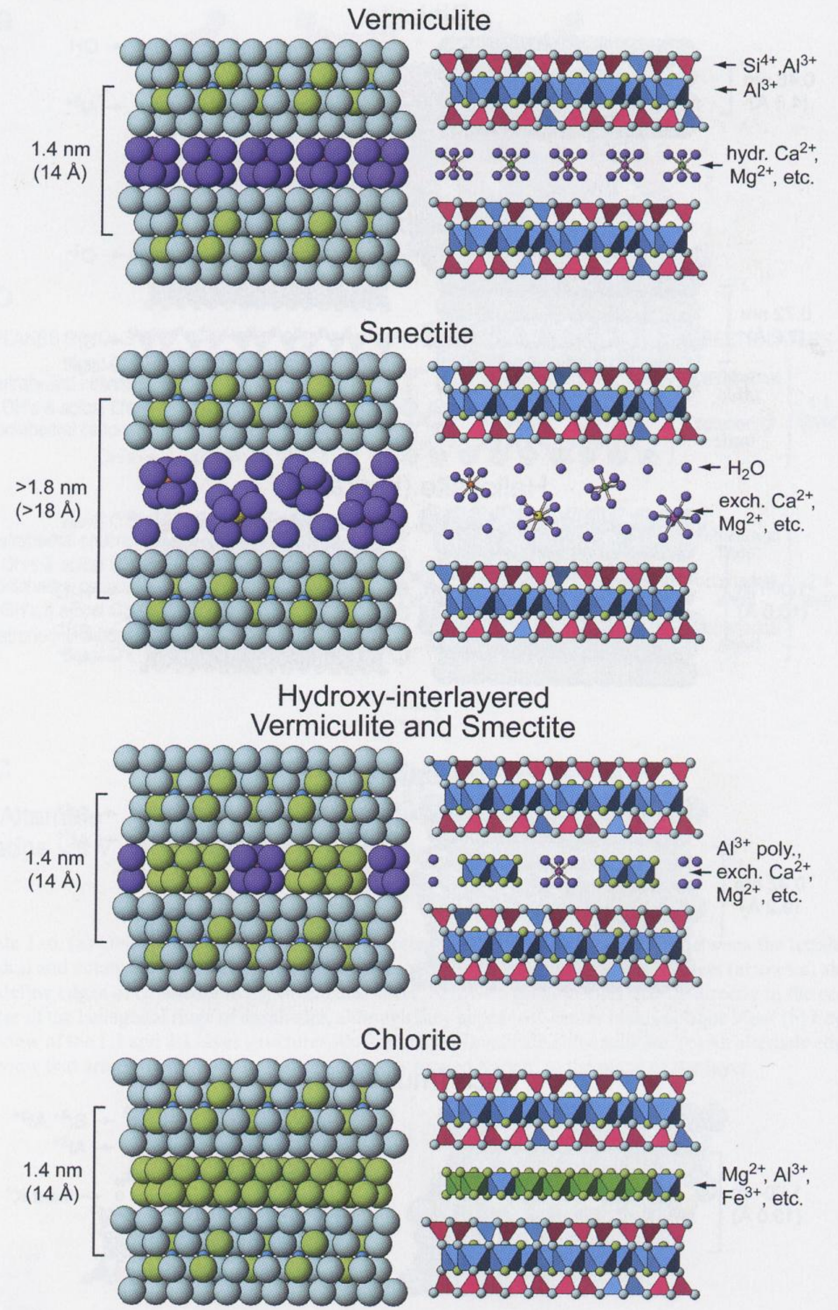

Vermiculite

Smectite

Hydroxy-interlayered Vermiculite and Smectite

Chlorite

te 1–7. Continued.

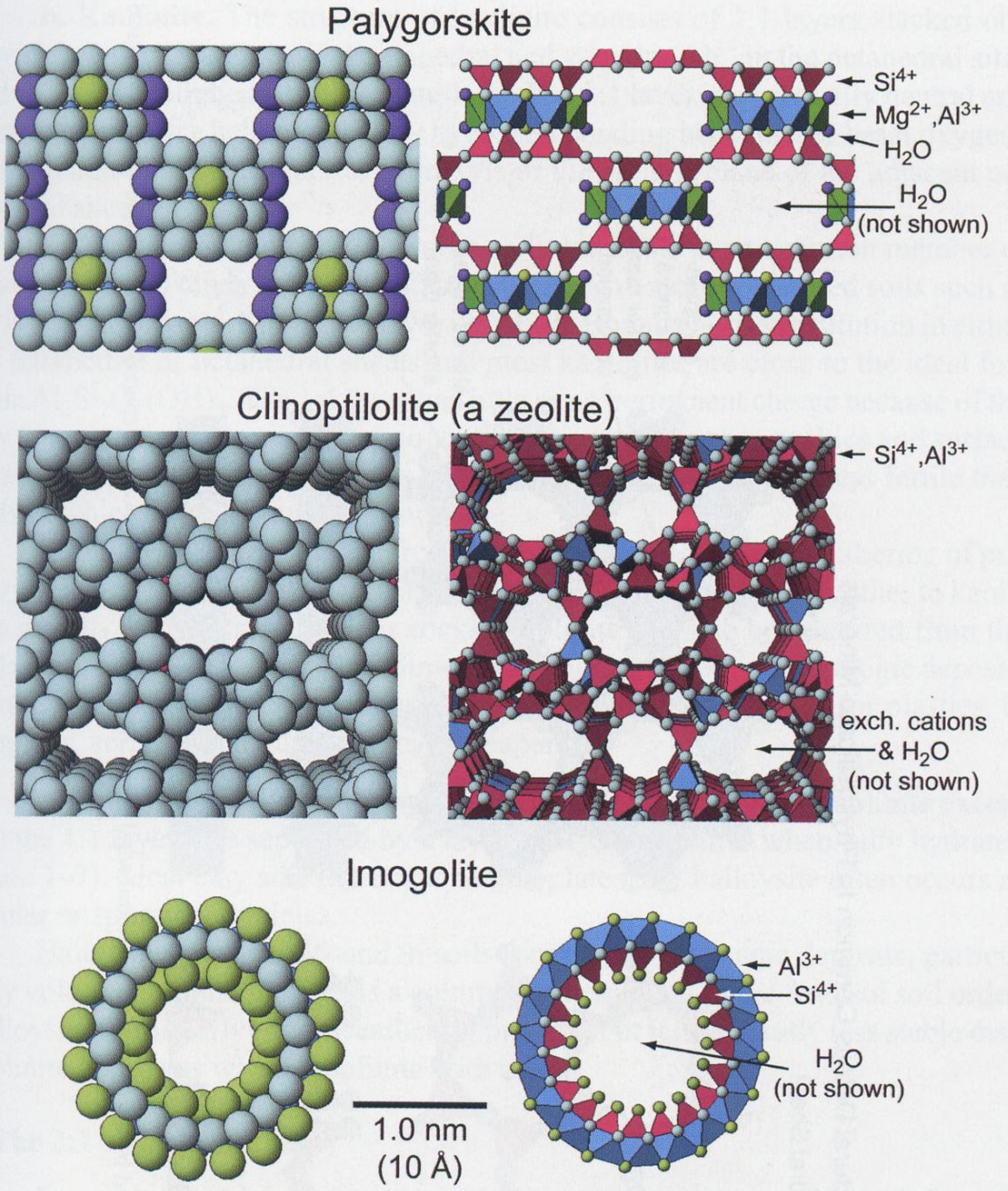

Plate 1–8. Structural models of representatives of three other aluminosilicate mineral groups that occur frequently in soils. All three are drawn to the same scale.

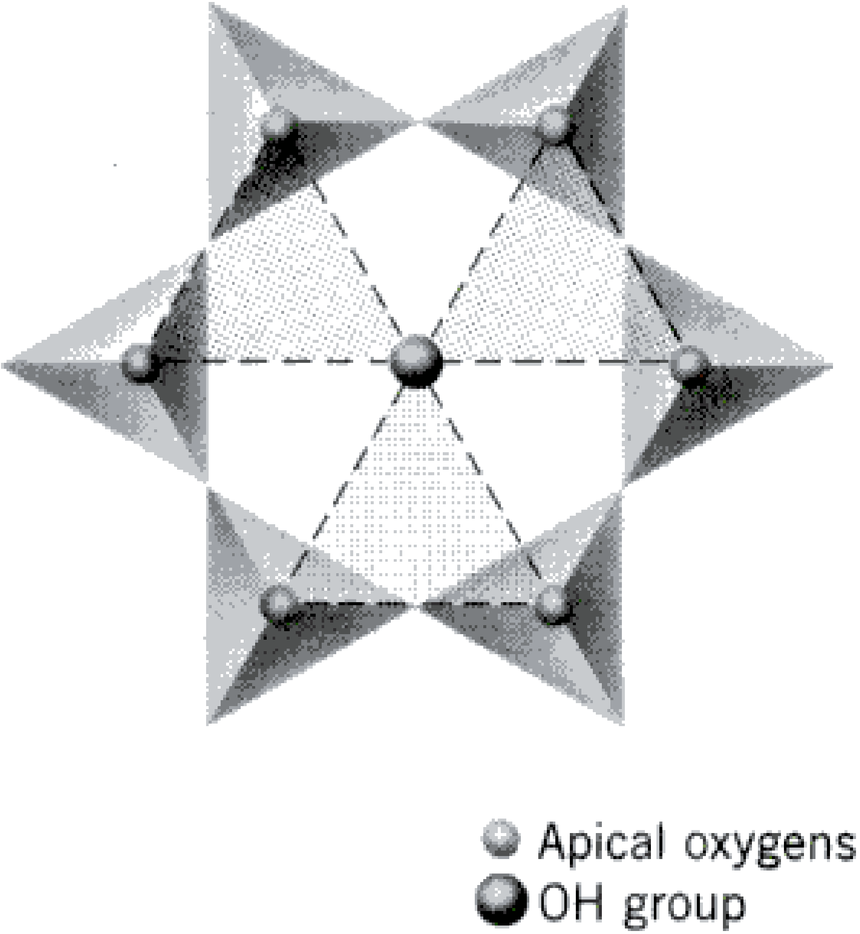

G. **18.29** Undistorted, hexagonal ring in an Si_2O_5 sheet owing the location of apical oxygens and (OH) group. In an ideal eet structure the size of the triangles (outlined by shading) is the me as the size of triangular faces of XO_6 octahedra.

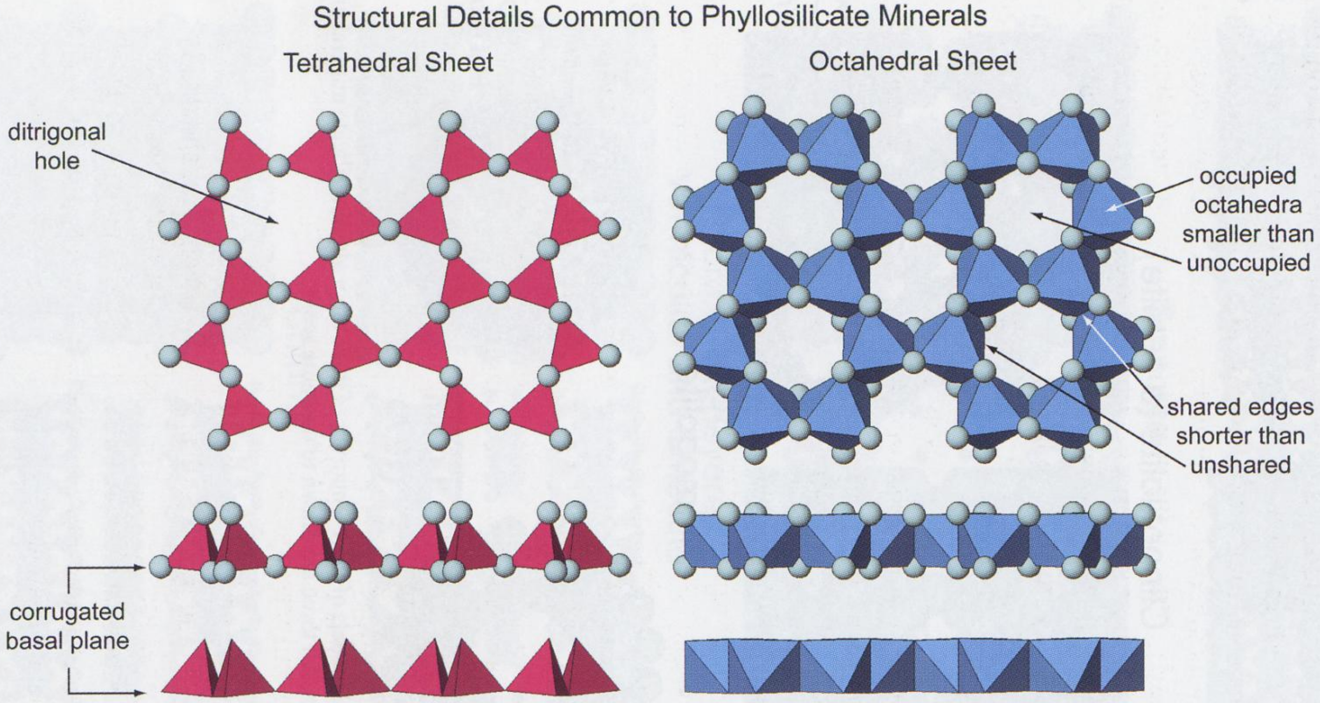

Plate 1–9. Structural details of phyllosilicates as illustrated by the octahedral and tetrahedral sheets of muscovite. Figures were prepared from the single-crystal structural refinement data of Rothbauer (1971).

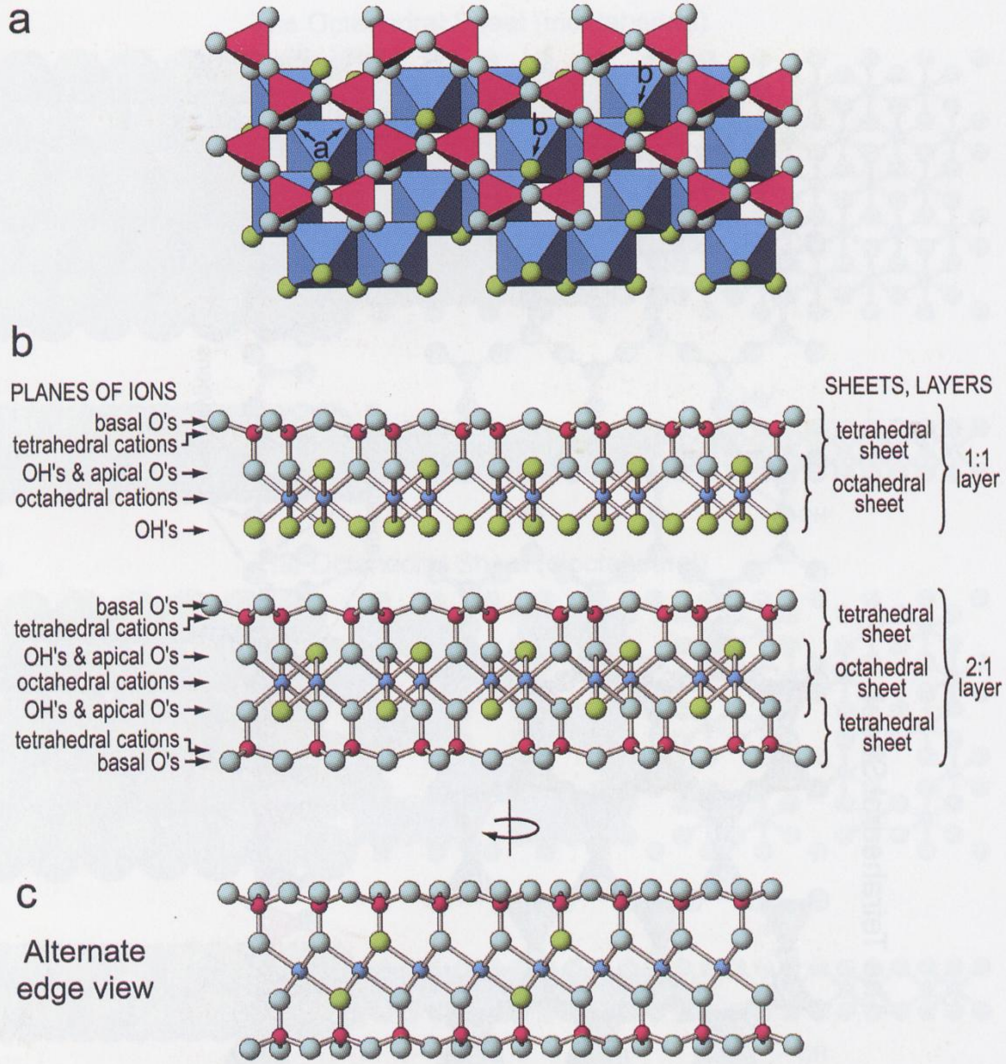

Plate 1–6. (a) Oblique view of the 1:1 layer structure illustrating the relationship between the tetrahedral and octahedral sheets. Note that adjacent apical oxygens of the tetrahedral sheet (arrows a) also define edges of octahedra in the octahedral sheet. Arrows b point to OHs that lie directly in the center of the hexagonal rings of tetrahedra, although they appear off-center in this oblique view. (b) Edge view of the 1:1 and 2:1 layer structures illustrating phyllosilicate nomenclature. (c) An alternate edge view that arises when the 2:1 structure above is rotated normal to the plane of the layer.

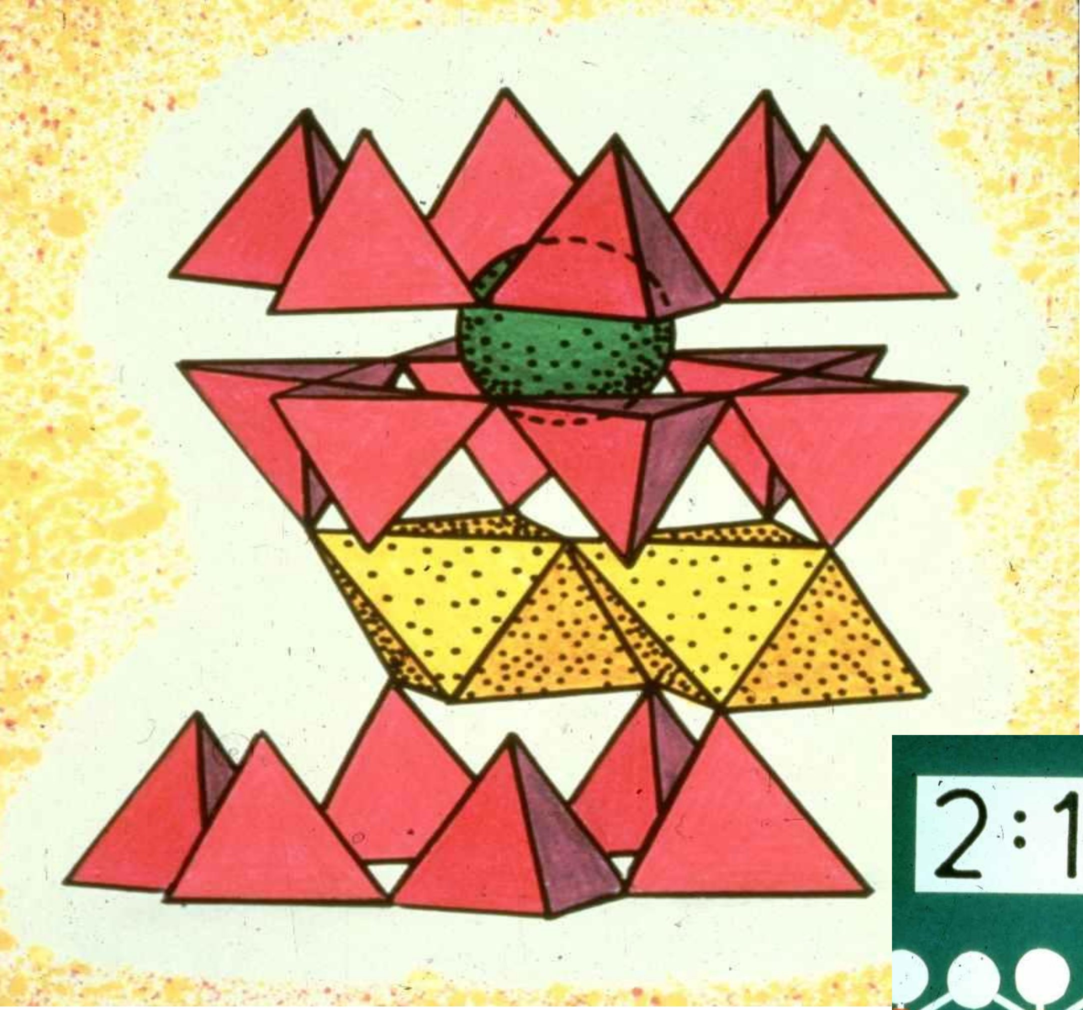

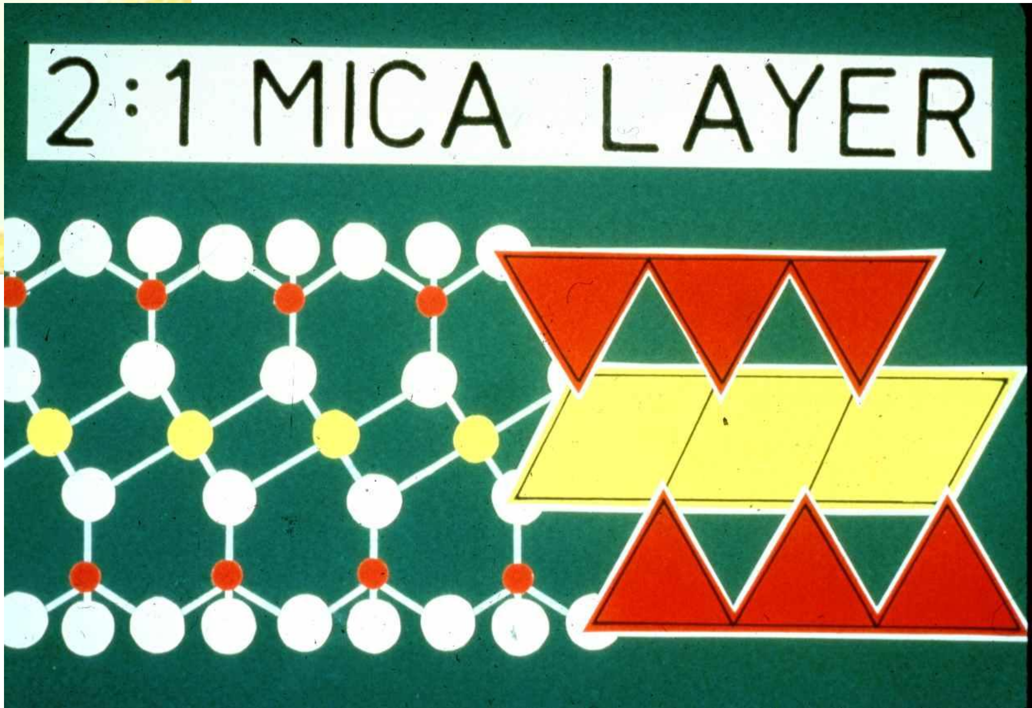

2:1 MICA LAYER

Diagrammatic sketch of the structure of chlorite (after Grim)

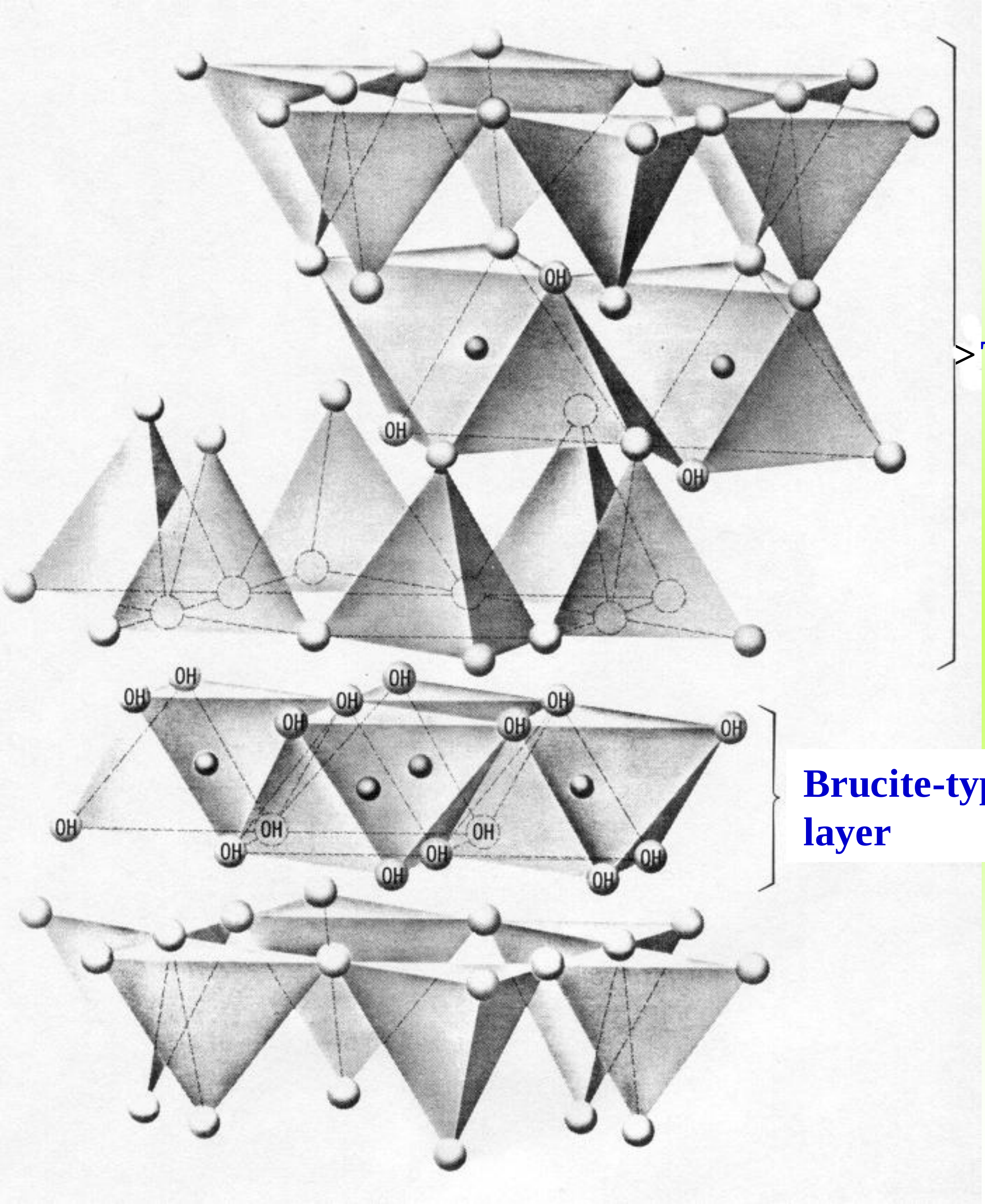

Talc Layer

Brucite-type layer

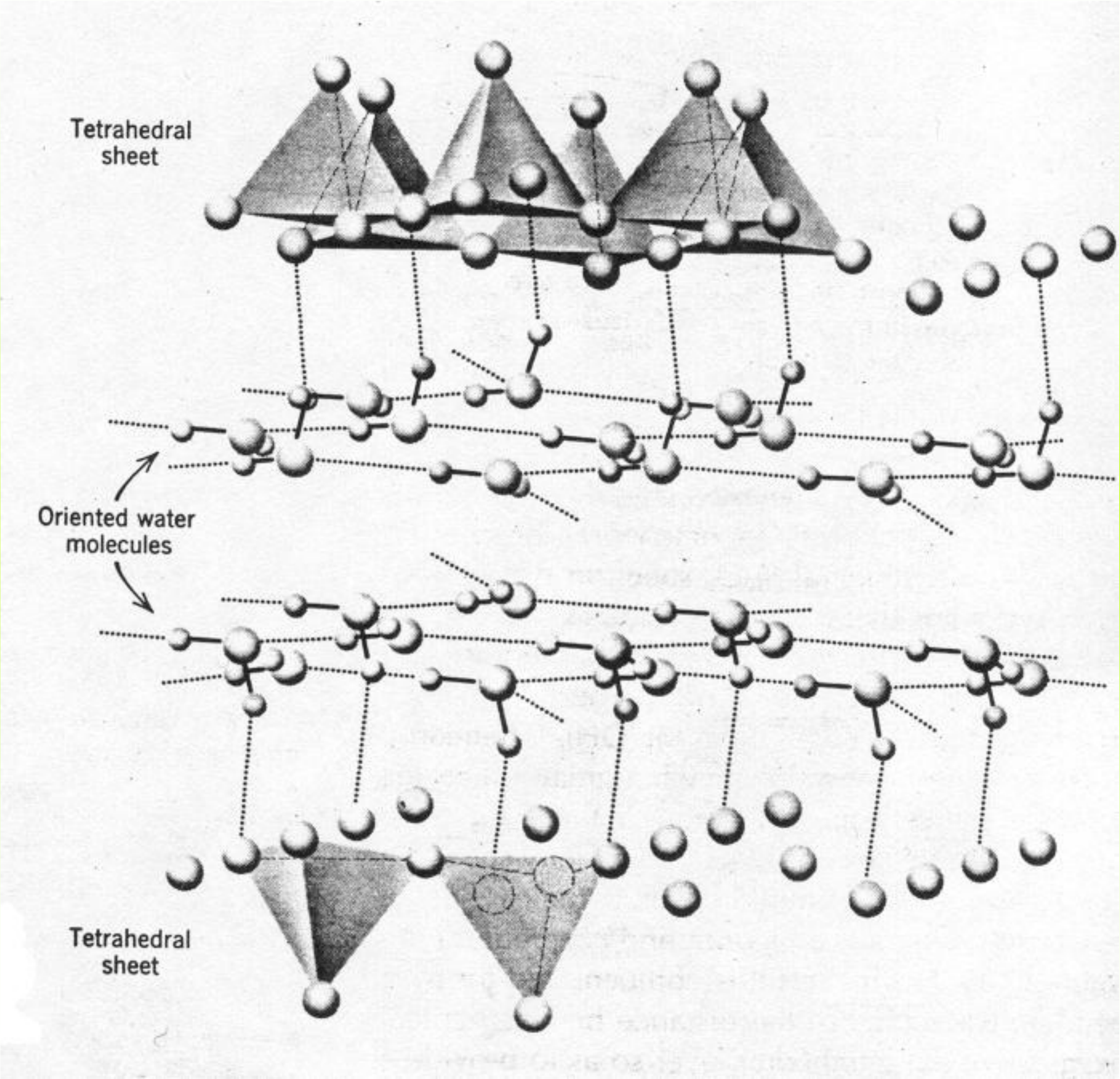

Diagrammatic sketch of the vermiculite structure, showing layers of water molecules (after Grim)

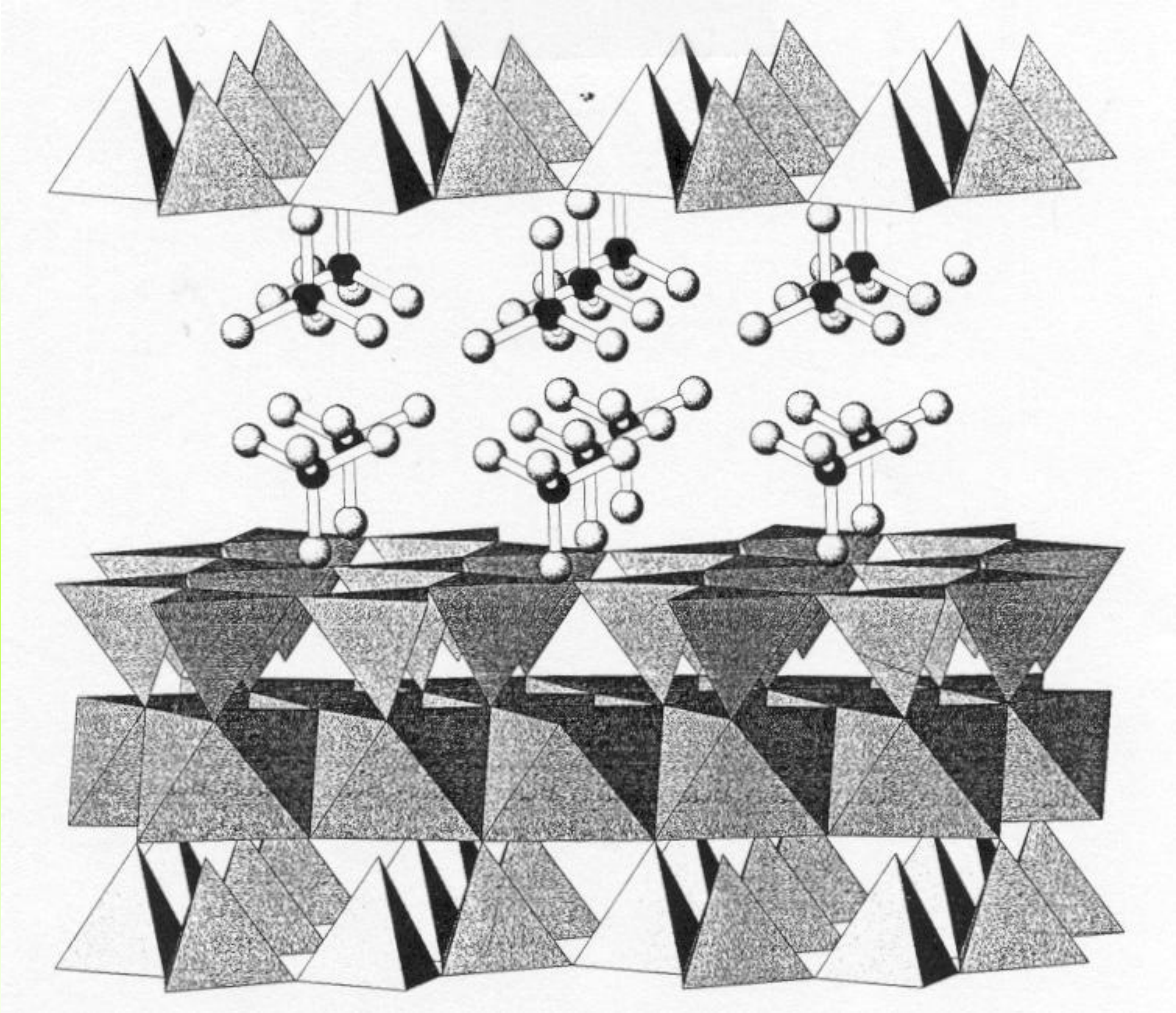

Average structure of tetramethylammonium-exchanged vermiculite.

Mixed-layer illite/smectite

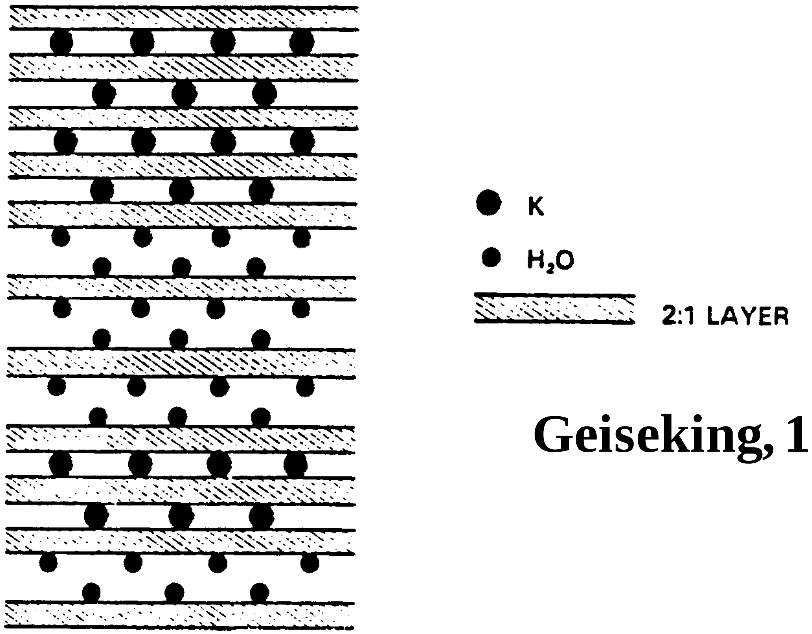

Geiseking, 1975

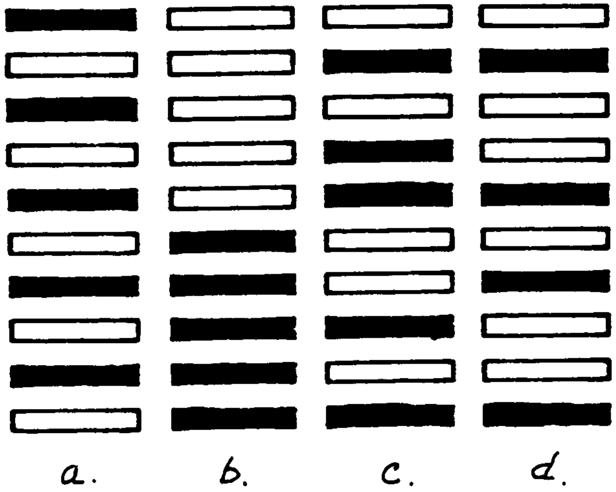

a REGULAR interstratification

b. SEGREGATED interstratification

c. RANDOM mixed

d. RAGULAR mixed

Triangular diagrams describing 2:1 layer silicates as three-way solid solutions with layer charge and location of layer charge as variables.

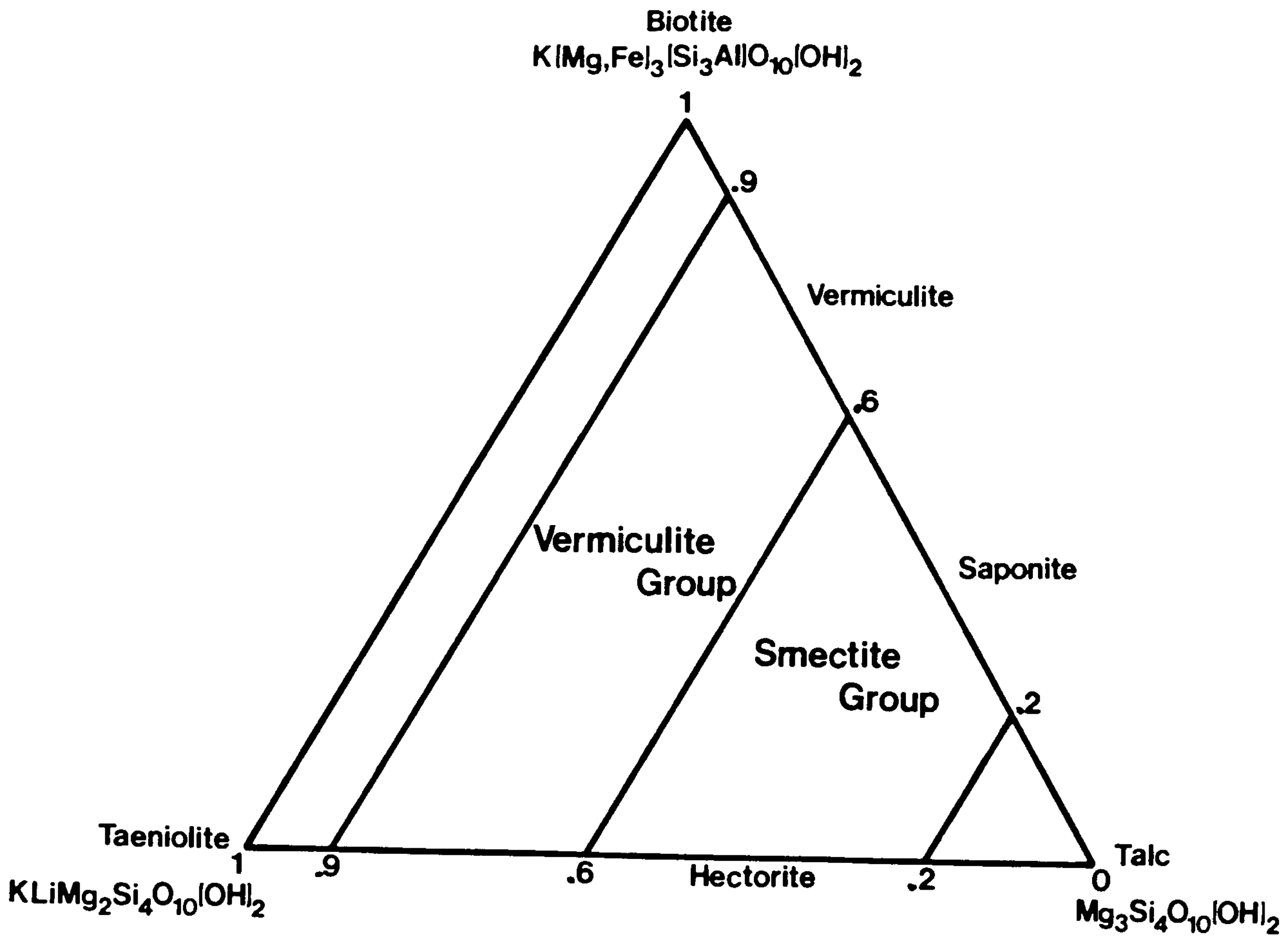

Triangular diagrams describing 2:1 layer silicates as three-way solid solutions with layer charge and location of layer charge as variables.

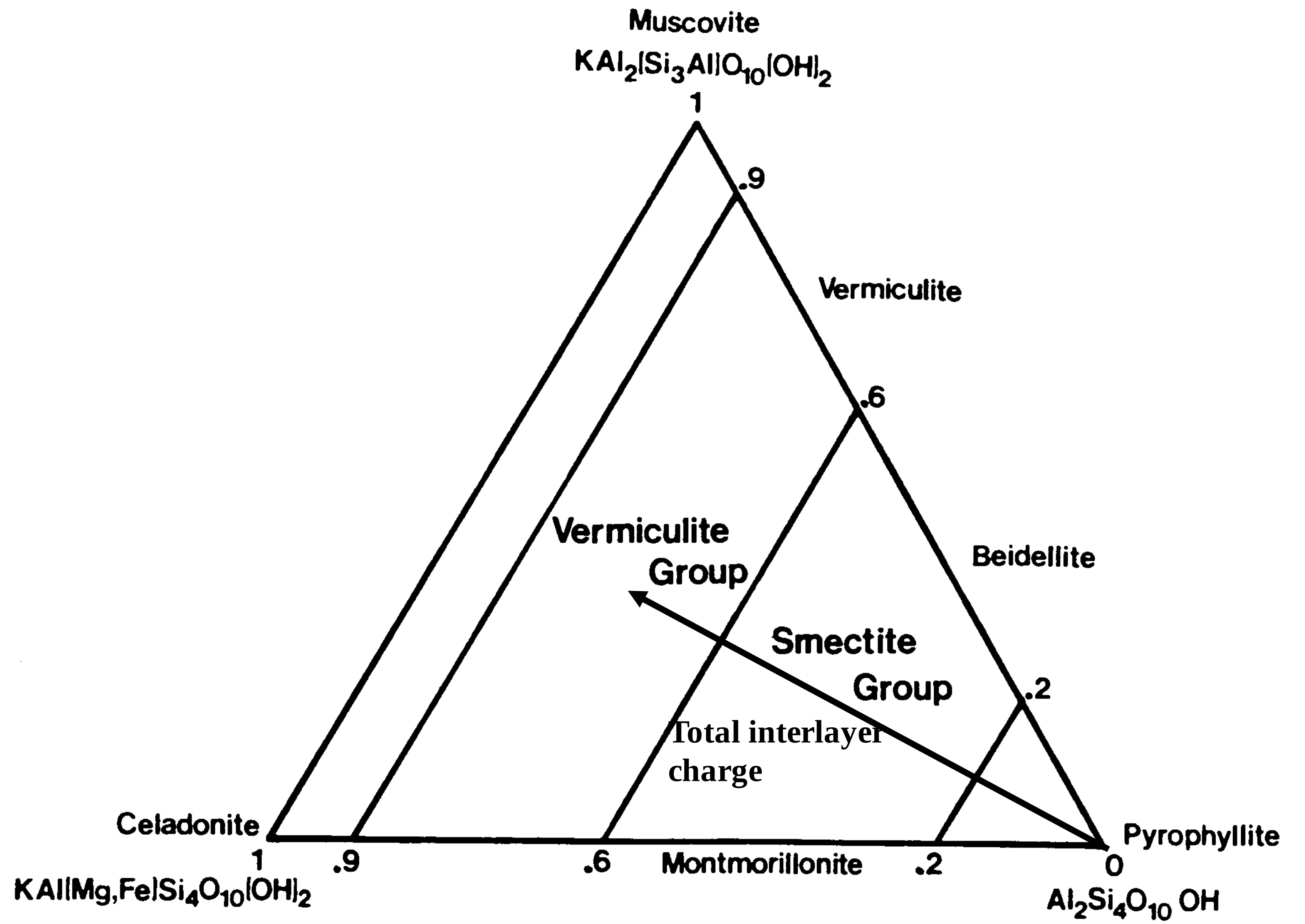

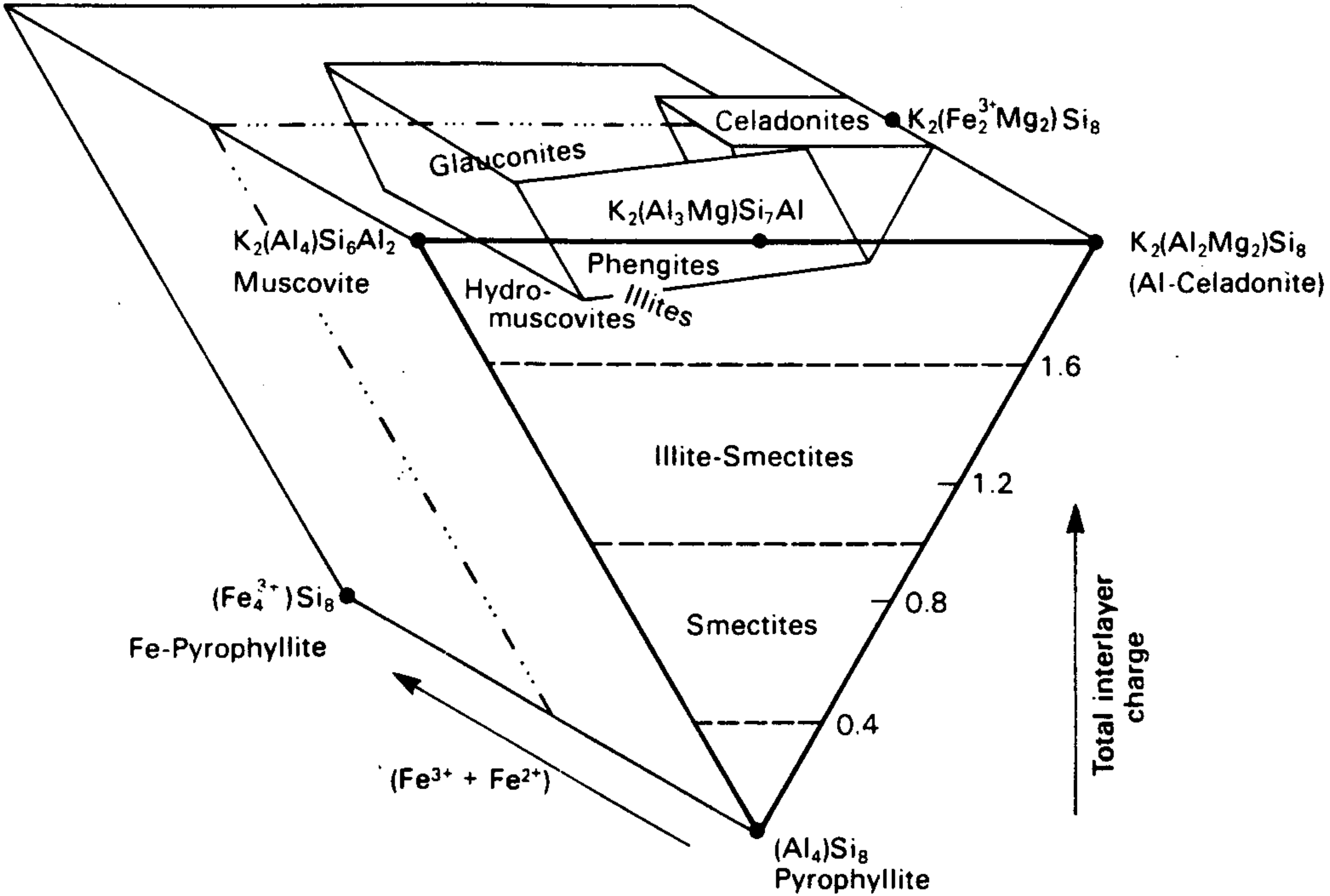

Dioctahedral 2:1 layer silicates: some ideal end-member compositions for the $O_{20}(OH)_4$ formula unit, and the compositional ranges for some micas, illites, illite-smectites and smectites.

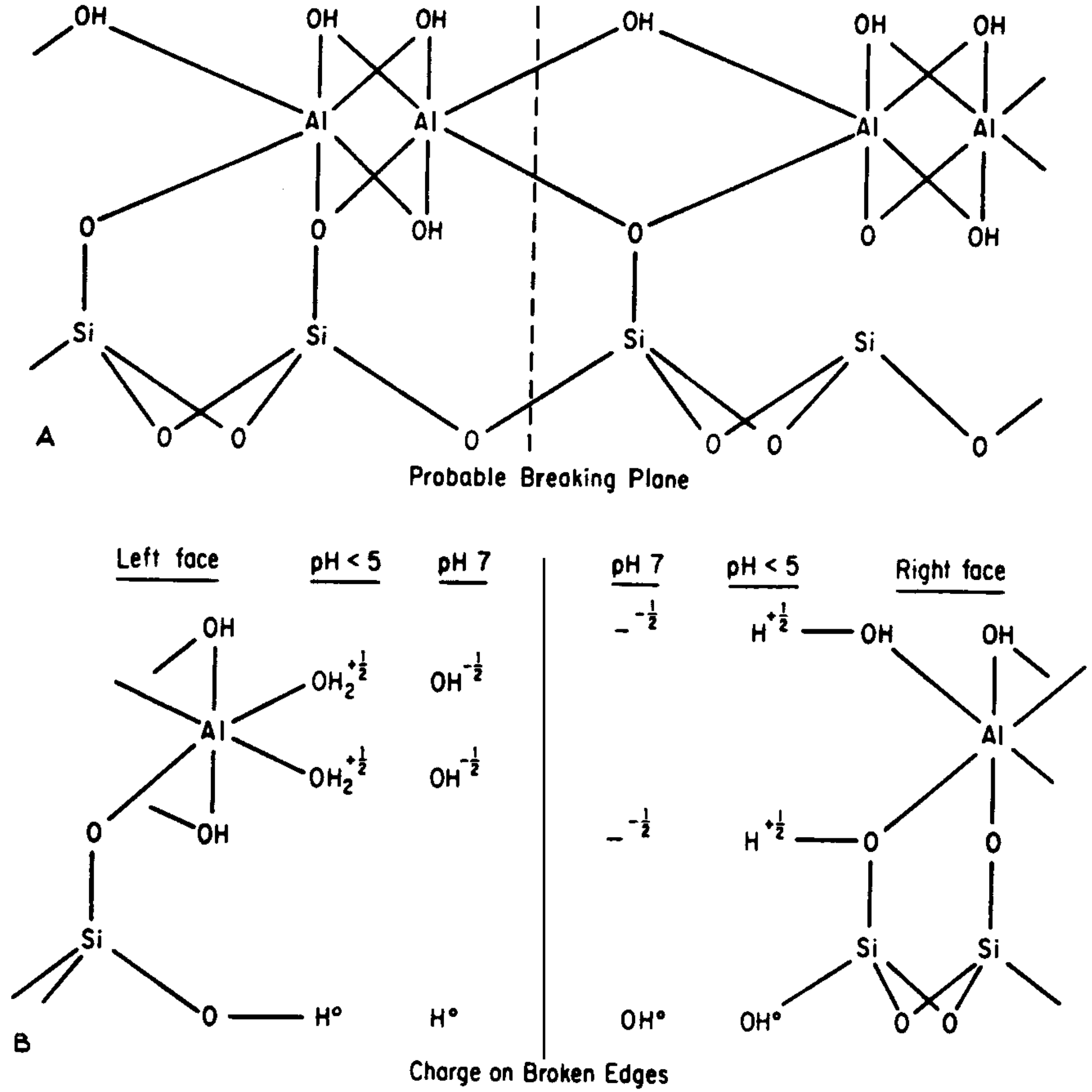

Kaolinite structure showing probable breaking plane and mechanism for edge charge by picking up H or OH from solution to give positive charge at low pH and negative charge at higher pH.

XRD treatments of the common silicate clay minerals.

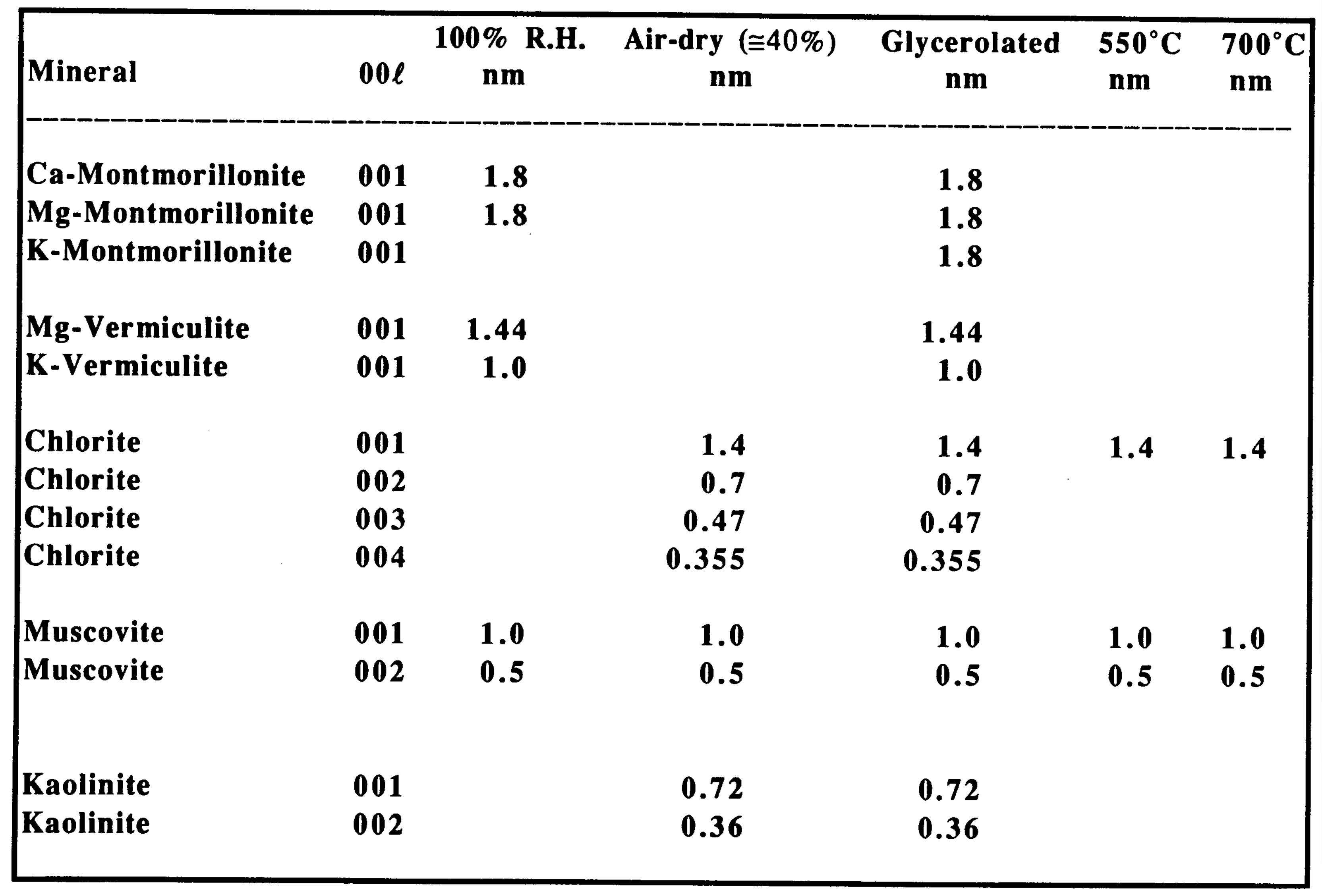

Mineral	00ℓ	100% R.H. nm	Air-dry (≅40%) nm	Glycerolated nm	550°C nm	700°C nm
Ca-Montmorillonite	001	1.8		1.8		
Mg-Montmorillonite	001	1.8		1.8		
K-Montmorillonite	001			1.8		
Mg-Vermiculite	001	1.44		1.44		
K-Vermiculite	001	1.0		1.0		
Chlorite	001		1.4	1.4	1.4	1.4
Chlorite	002		0.7	0.7		
Chlorite	003		0.47	0.47		
Chlorite	004		0.355	0.355		
Muscovite	001	1.0	1.0	1.0	1.0	1.0
Muscovite	002	0.5	0.5	0.5	0.5	0.5
Kaolinite	001		0.72	0.72		
Kaolinite	002		0.36	0.36		

Classification and generalized structural formulae of phyllosilicates

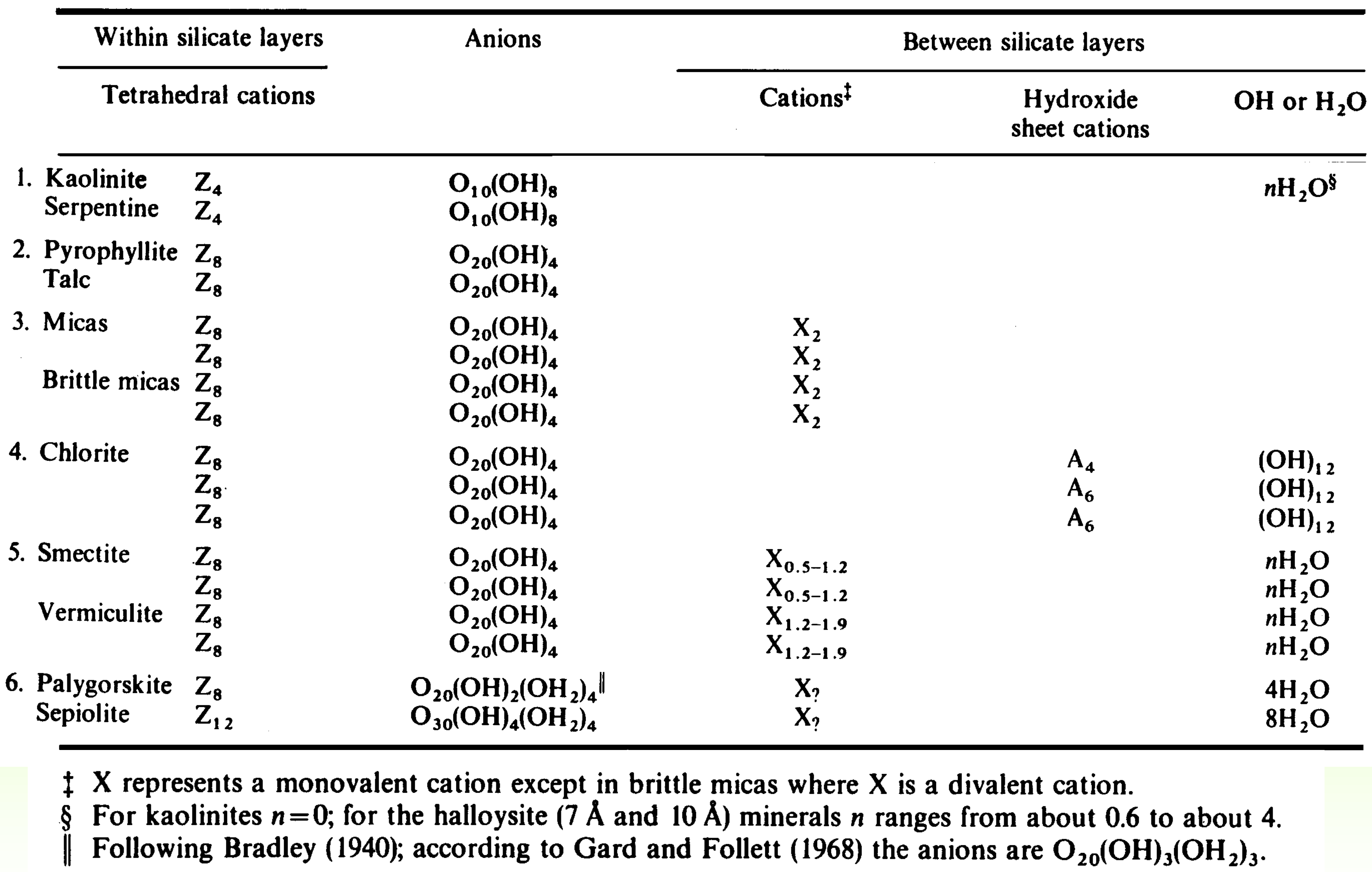

	Within silicate layers	Anions	Between silicate layers		
	Tetrahedral cations		Cations‡	Hydroxide sheet cations	OH or H_2O
1. Kaolinite	Z_4	$O_{10}(OH)_8$			nH_2O§
Serpentine	Z_4	$O_{10}(OH)_8$			
2. Pyrophyllite	Z_8	$O_{20}(OH)_4$			
Talc	Z_8	$O_{20}(OH)_4$			
3. Micas	Z_8	$O_{20}(OH)_4$	X_2		
	Z_8	$O_{20}(OH)_4$	X_2		
Brittle micas	Z_8	$O_{20}(OH)_4$	X_2		
	Z_8	$O_{20}(OH)_4$	X_2		
4. Chlorite	Z_8	$O_{20}(OH)_4$		A_4	$(OH)_{12}$
	Z_8	$O_{20}(OH)_4$		A_6	$(OH)_{12}$
	Z_8	$O_{20}(OH)_4$		A_6	$(OH)_{12}$
5. Smectite	Z_8	$O_{20}(OH)_4$	$X_{0.5-1.2}$		nH_2O
	Z_8	$O_{20}(OH)_4$	$X_{0.5-1.2}$		nH_2O
Vermiculite	Z_8	$O_{20}(OH)_4$	$X_{1.2-1.9}$		nH_2O
	Z_8	$O_{20}(OH)_4$	$X_{1.2-1.9}$		nH_2O
6. Palygorskite	Z_8	$O_{20}(OH)_2(OH_2)_4$‖	$X_?$		$4H_2O$
Sepiolite	Z_{12}	$O_{30}(OH)_4(OH_2)_4$	$X_?$		$8H_2O$

‡ X represents a monovalent cation except in brittle micas where X is a divalent cation.

§ For kaolinites $n=0$; for the halloysite (7 Å and 10 Å) minerals n ranges from about 0.6 to about 4.

‖ Following Bradley (1940); according to Gard and Follett (1968) the anions are $O_{20}(OH)_3(OH_2)_3$.

Nature of octahedral sheet and negative charge of phyllosilicates.

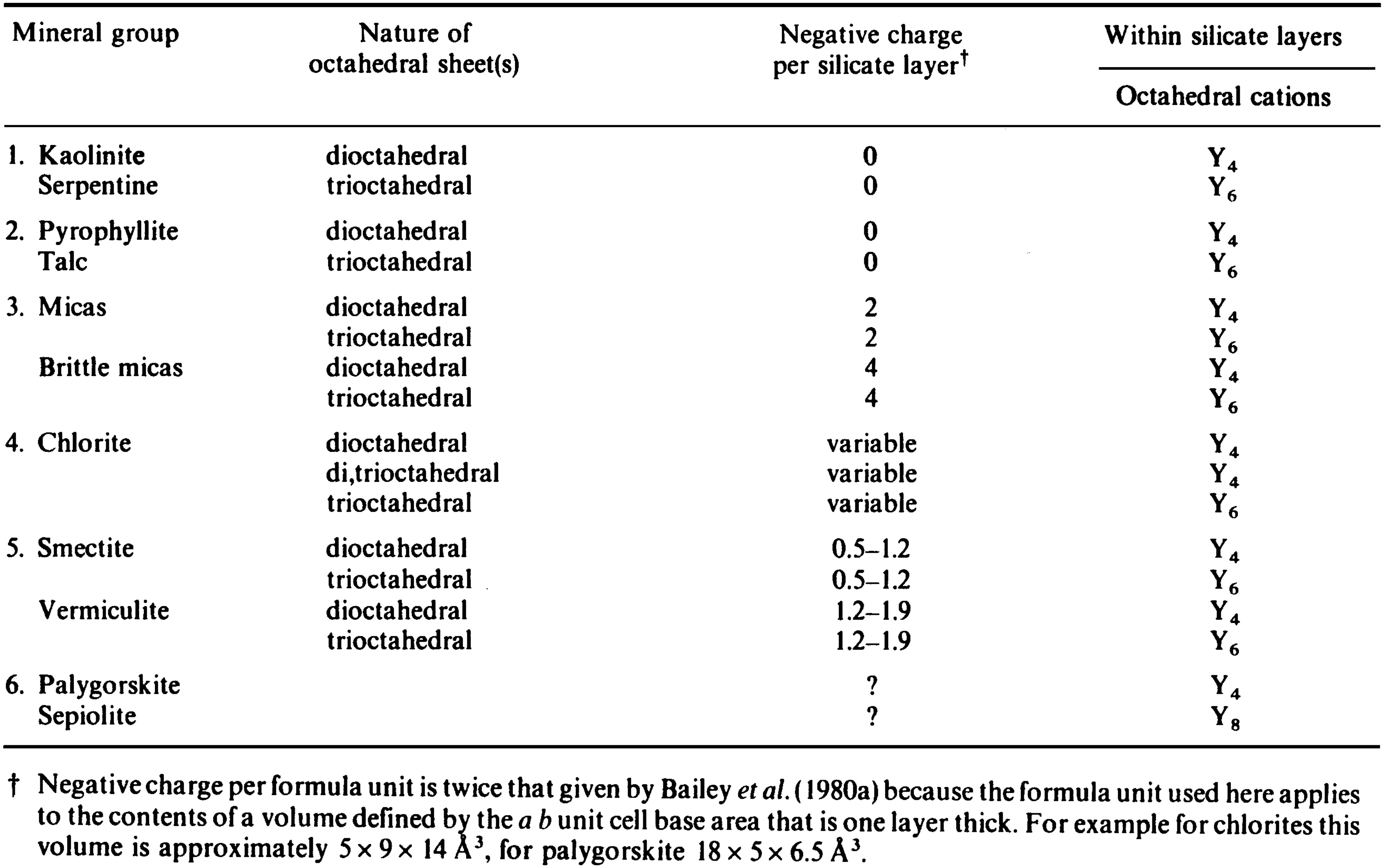

Mineral group	Nature of octahedral sheet(s)	Negative charge per silicate layer†	Within silicate layers
			Octahedral cations
1. Kaolinite	dioctahedral	0	Y_4
Serpentine	trioctahedral	0	Y_6
2. Pyrophyllite	dioctahedral	0	Y_4
Talc	trioctahedral	0	Y_6
3. Micas	dioctahedral	2	Y_4
	trioctahedral	2	Y_6
Brittle micas	dioctahedral	4	Y_4
	trioctahedral	4	Y_6
4. Chlorite	dioctahedral	variable	Y_4
	di,trioctahedral	variable	Y_4
	trioctahedral	variable	Y_6
5. Smectite	dioctahedral	0.5–1.2	Y_4
	trioctahedral	0.5–1.2	Y_6
Vermiculite	dioctahedral	1.2–1.9	Y_4
	trioctahedral	1.2–1.9	Y_6
6. Palygorskite		?	Y_4
Sepiolite		?	Y_8

† Negative charge per formula unit is twice that given by Bailey *et al.* (1980a) because the formula unit used here applies to the contents of a volume defined by the *a b* unit cell base area that is one layer thick. For example for chlorites this volume is approximately $5 \times 9 \times 14$ Å^3, for palygorskite $18 \times 5 \times 6.5$ Å^3.

Atoms per structural unit for clintonite

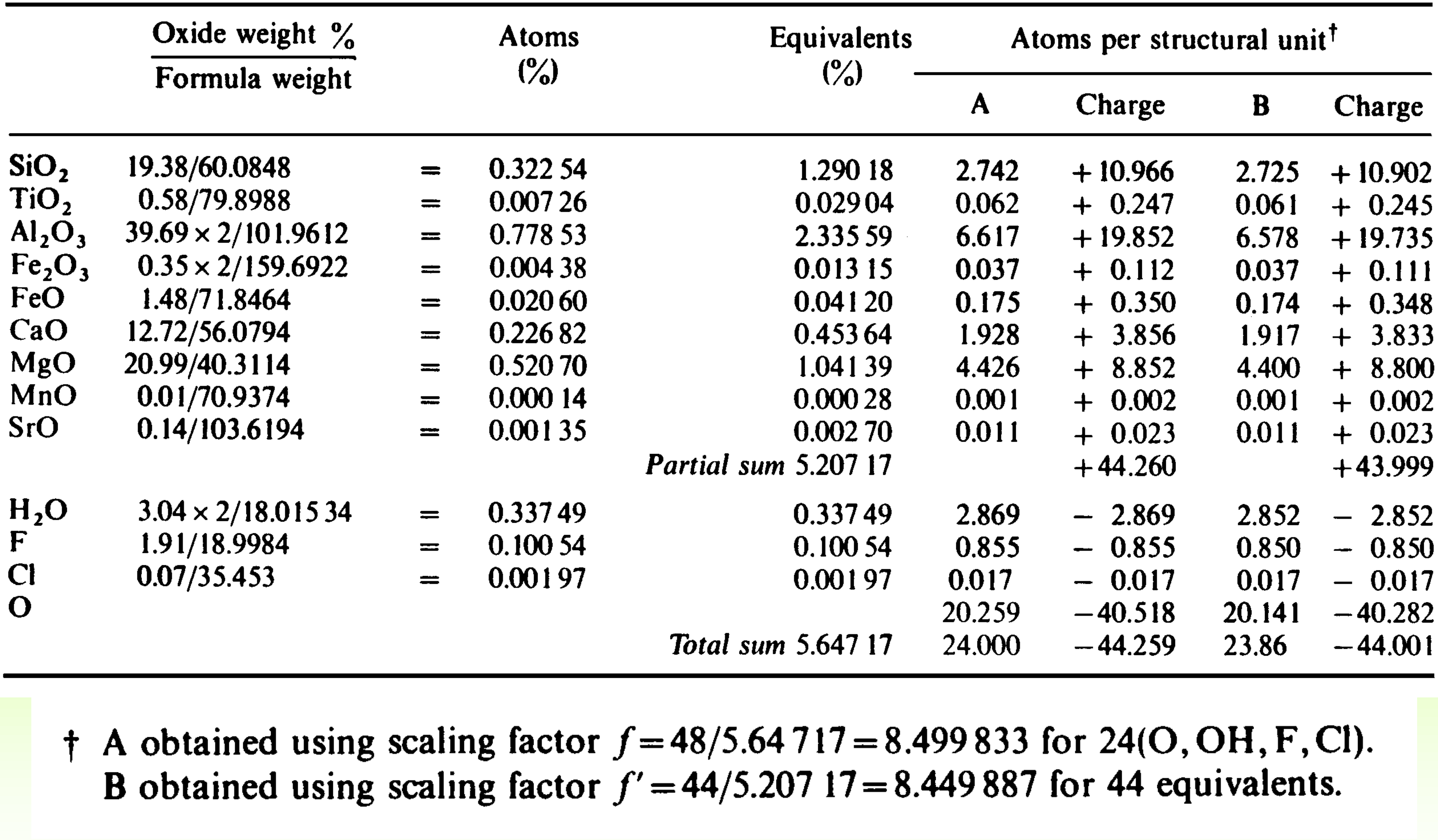

	Oxide weight % / Formula weight		Atoms (%)	Equivalents (%)	Atoms per structural unit†			
					A	Charge	B	Charge
SiO_2	19.38/60.0848	=	0.322 54	1.290 18	2.742	+10.966	2.725	+10.902
TiO_2	0.58/79.8988	=	0.007 26	0.029 04	0.062	+ 0.247	0.061	+ 0.245
Al_2O_3	39.69 × 2/101.9612	=	0.778 53	2.335 59	6.617	+19.852	6.578	+19.735
Fe_2O_3	0.35 × 2/159.6922	=	0.004 38	0.013 15	0.037	+ 0.112	0.037	+ 0.111
FeO	1.48/71.8464	=	0.020 60	0.041 20	0.175	+ 0.350	0.174	+ 0.348
CaO	12.72/56.0794	=	0.226 82	0.453 64	1.928	+ 3.856	1.917	+ 3.833
MgO	20.99/40.3114	=	0.520 70	1.041 39	4.426	+ 8.852	4.400	+ 8.800
MnO	0.01/70.9374	=	0.000 14	0.000 28	0.001	+ 0.002	0.001	+ 0.002
SrO	0.14/103.6194	=	0.001 35	0.002 70	0.011	+ 0.023	0.011	+ 0.023
				Partial sum 5.207 17		+44.260		+43.999
H_2O	3.04 × 2/18.015 34	=	0.337 49	0.337 49	2.869	− 2.869	2.852	− 2.852
F	1.91/18.9984	=	0.100 54	0.100 54	0.855	− 0.855	0.850	− 0.850
Cl	0.07/35.453	=	0.001 97	0.001 97	0.017	− 0.017	0.017	− 0.017
O					20.259	−40.518	20.141	−40.282
				Total sum 5.647 17	24.000	−44.259	23.86	−44.001

† A obtained using scaling factor $f = 48/5.64\,717 = 8.499\,833$ for 24(O, OH, F, Cl).
B obtained using scaling factor $f' = 44/5.207\,17 = 8.449\,887$ for 44 equivalents.

$[\mathrm{Si}_{2.74}\,\mathrm{Al}_{5.26}]\,[\mathrm{Al}_{1.36}\,\mathrm{Fe}_{0.04}{}^{3+}\,\mathrm{Fe}_{0.18}{}^{2+}\,\mathrm{Mg}_{4.43}]\ \Sigma 1.93$

Ca is divalent 1.93 x 2 = 3.86

Total cations ideal 8 Si x 4 = 32

4 Al or 6 Mg = 12

IDEAL}

TOTAL cations 44

Tetrahedral charge deficit - 5.26

Octahedral charge excess + 1.40

Overall charge deficit - 3.86

(2.74 x 4) + (5.26 x 3) + (1.36 x 3) (0.04 x 3) + (0.18 x 2) + (4.43 x 2) =

10.96 + 15.78 + 4.08 + 0.12 + 0.36 + 8.86 = 40.16

Actual total + 40.14; Charge Deficit - 3.86

$$C_i = 1000\ \zeta\ /M$$

C_i= potential interlamellar cation exchange capacity (meq/g)

ζ = cation density, equivalent /mol for half or one unit cell.

M = Mean molecular mass (without exchangeable cations) calculated for typical composition, or the mineral with known chemical composition .

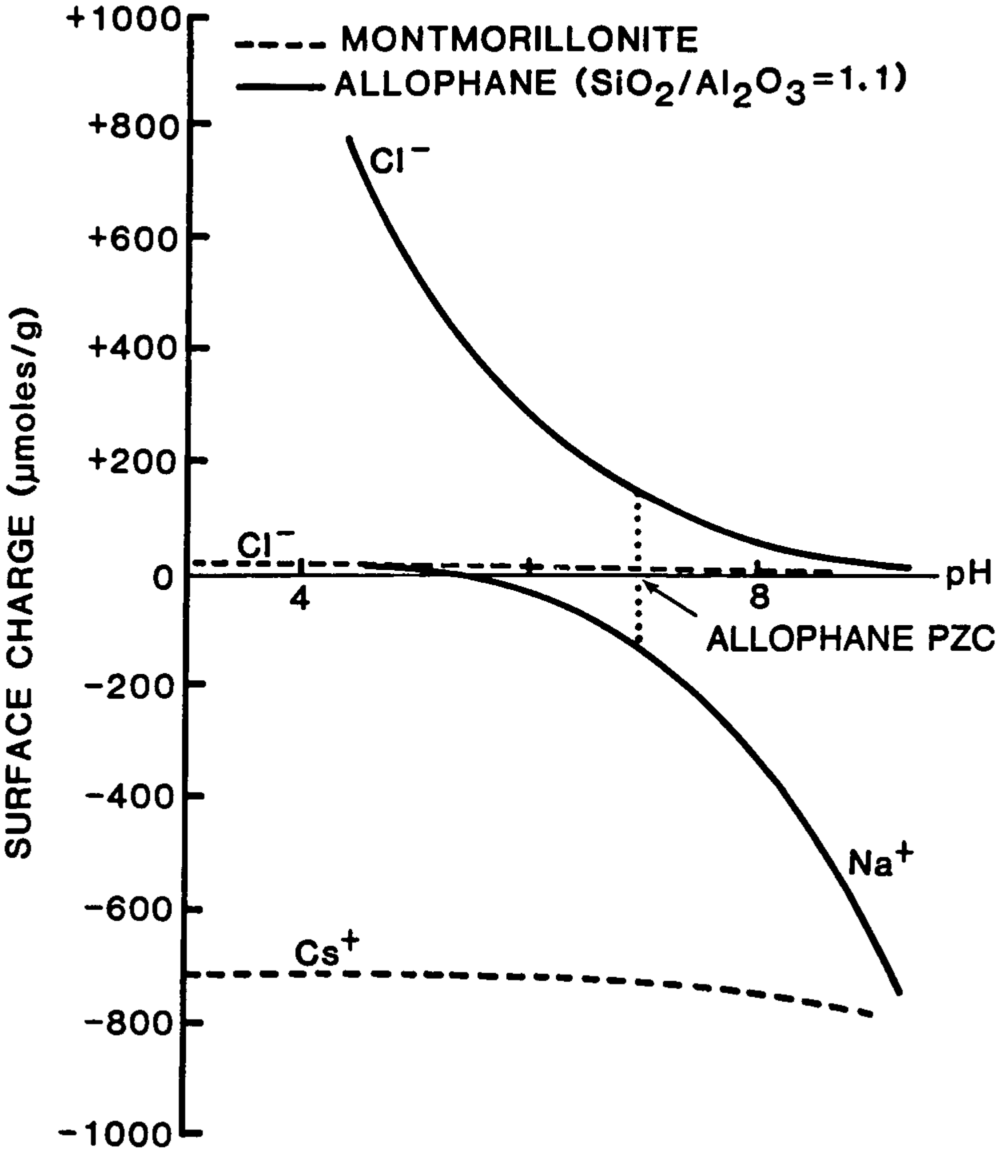

pH dependence of surface charge on allophane and montmorillonite, measured from the adsorption of cations and anions in 0.1 *M* CsCl, respectively. (Data taken from Greenland, 1974; Clark & McBride, 1984a).

Approximate layer charge of 2:1 phyllosilicates

Mineral	Layer charge[1] per half unit cell $[O_{10}(OH)_2]$	Mean molecular mass (M)[2] $[O_{10}(OH)_2]$	Interlayer CEC $cmol\ kg^{-1}$
Hectorite	0.20-0.25	380	50-65
Montmorillonite	0.25-0.40	360	70-110
Vermiculite	0.50-0.80	390	130-210
Illite	0.60-0.90	385	160-230
Biotite	~ 1.00	450	~ 220
Muscovite	~ 1.00	390	~ 260

[1] Without exchangeable cations and calculated for typical composition (Lagaly, 1994, corrected).

[2] Formula weight.

(See A. R. Mermut.1994. Layer charge characteristics of 2:1 silicate caly minerals. CMS Workshop lectures vol. 6 CMS Society.

Summary of the elemental composition of the source clay mineral

	KGa-1	KGa-2	SWy-2	SAz-1	Syn-1
SiO_2	43.36	43.49	61.64	59.65	49.77
SE	0.39	0.19	1.29	0.16	0.32
Al_2O_3	38.58	38.14	22.05	19.98	38.56
SE	0.24	0.14	0.19	0.00	0.03
Fe_2O_3	0.35	1.15	4.37	1.77	0.12
SE	0.02	0.02	0.06	0.03	0.02
TiO_2	1.67	1.91	0.009	0.25	0.03
SE	0.01	0.03	0.00	0.01	0.00
MgO	0.04	0.04	2.94	6.73	0.18
SE	0.01	0.01	0.02	0.03	0.00
CaO	0.04	0.03	1.18	3.15	0.05
SE	0.01	0.01	0.03	0.04	0.00
N_2O	0.05	0.06	1.47	0.06	0.08
SE	0.01	0.01	0.03	0.01	0.01
K_2O	0.00	0.02	0.20	0.19	0.00
SE	0.00	0.00	0.01	0.01	0.00
P_2O_5	0.37	0.32	0.00	0.01	0.00
SE	0.03	0.00	0.00	0.00	0.00
Ignition loss 110-550°C	13.60	13.30	0.61	4.58	8.65
Ignition loss 550-1000°C	1.45	1.73	5.15	3.59	2.18
Total	99.51	100.19	99.52	99.95	99.61

(Mermut and Faz-Cano, 2001; Clays and Clay Minerals); SE standard error

Structural formula of the source clay minerals

	KGa-1	KGa-2	SWy-2	SAz-1	Syn-1
Si	3.85	3.84	7.89	7.86	6.50
Al	0.15	0.16	0.11	0.14	1.50
Σ tet.	4.00	4.00	8.00	8.00	8.00
Al	3.88	3.80	3.23	2.96	4.44
Ti	0.10	0.13		0.02	
Fe^{3+}	0.02	0.07	0.42	0.18	0.01
Mg			0.56	1.32	0.04
Σ oct.	4.00	4.00	4.21	4.48	4.49
Ca	0.005	0.005	0.52	0.88	0.007
Na	0.009	0.01	0.14	0.01	0.01
K		0.002	0.01	0.05	

(Mermut and Faz-Cano, 2001; Clays and Clay Minerals)

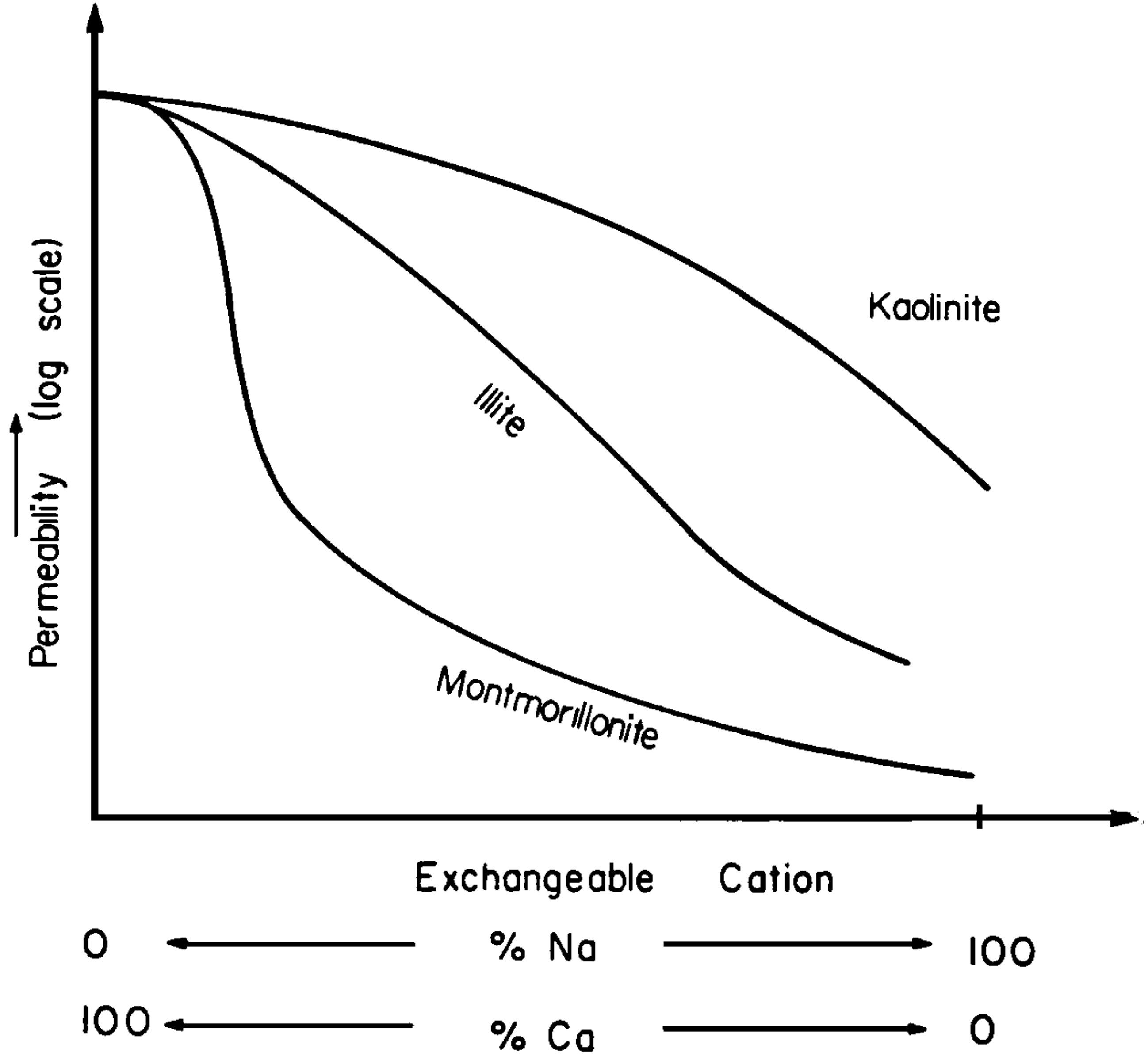

Influence of exchangeable cations on permeability of different clays.

Edge-view sketches to show relative size and shape of clay particles; dimension not shown is equal to length.

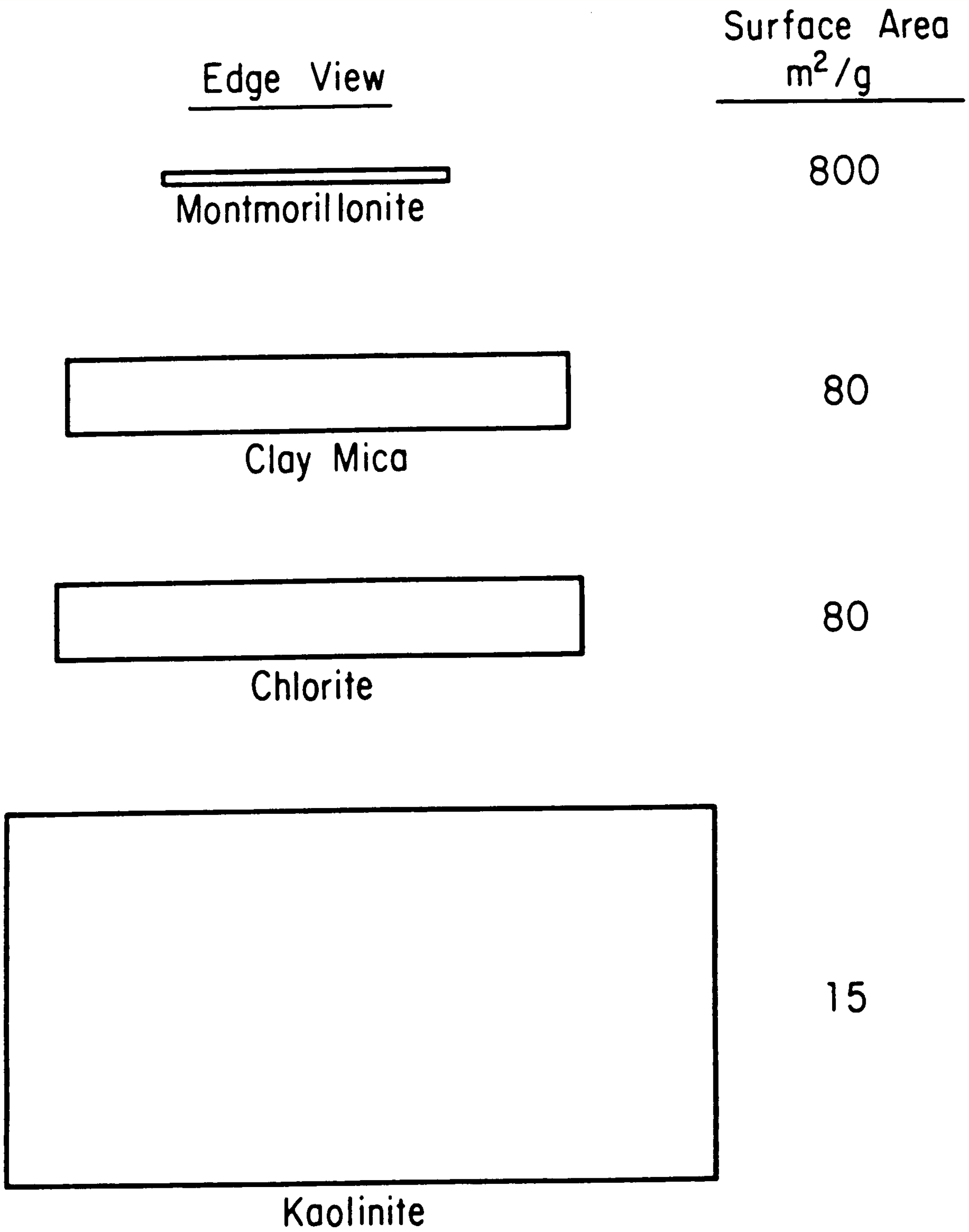

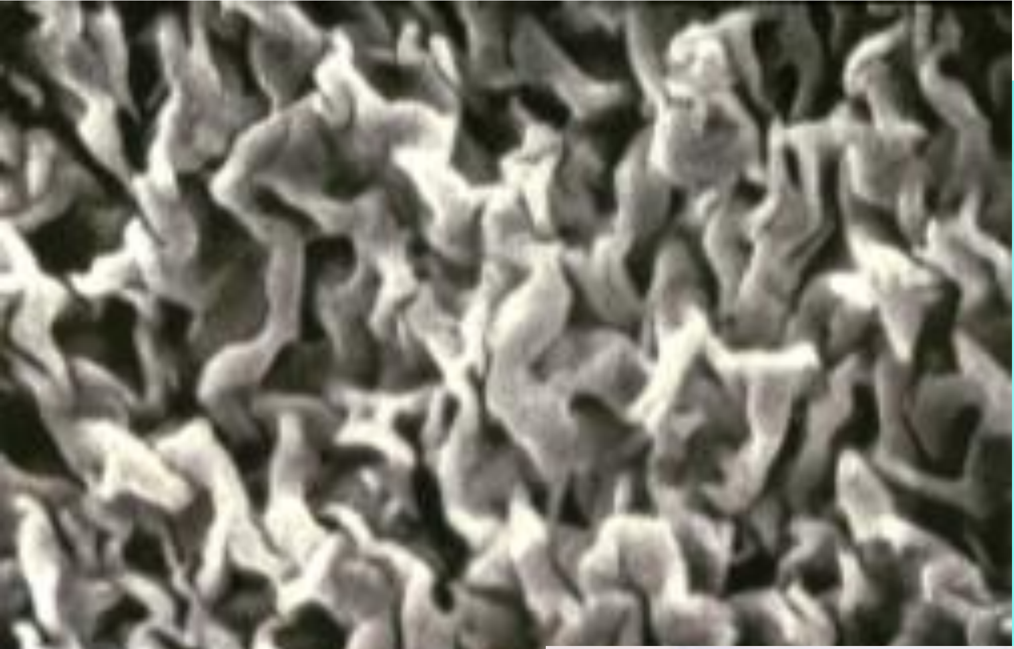

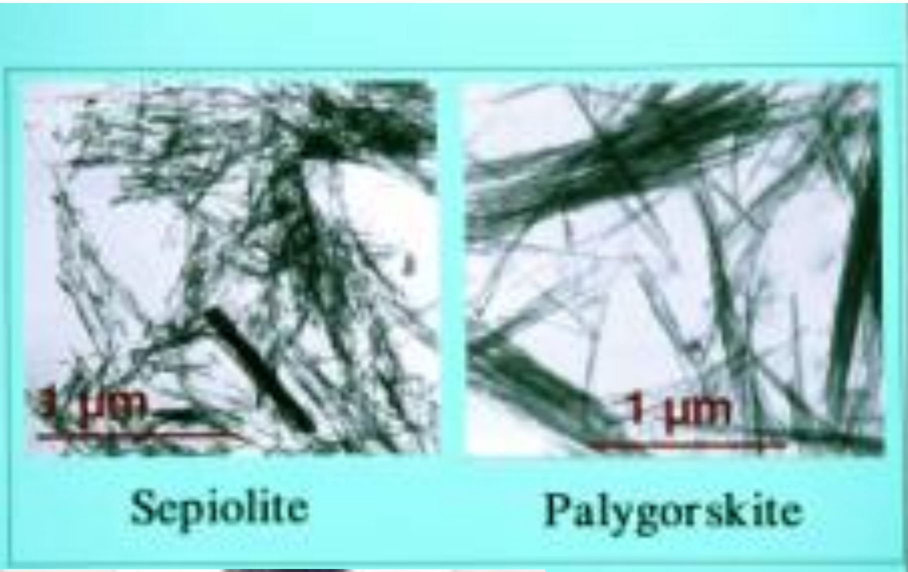

Sepiolite **Palygorskite**

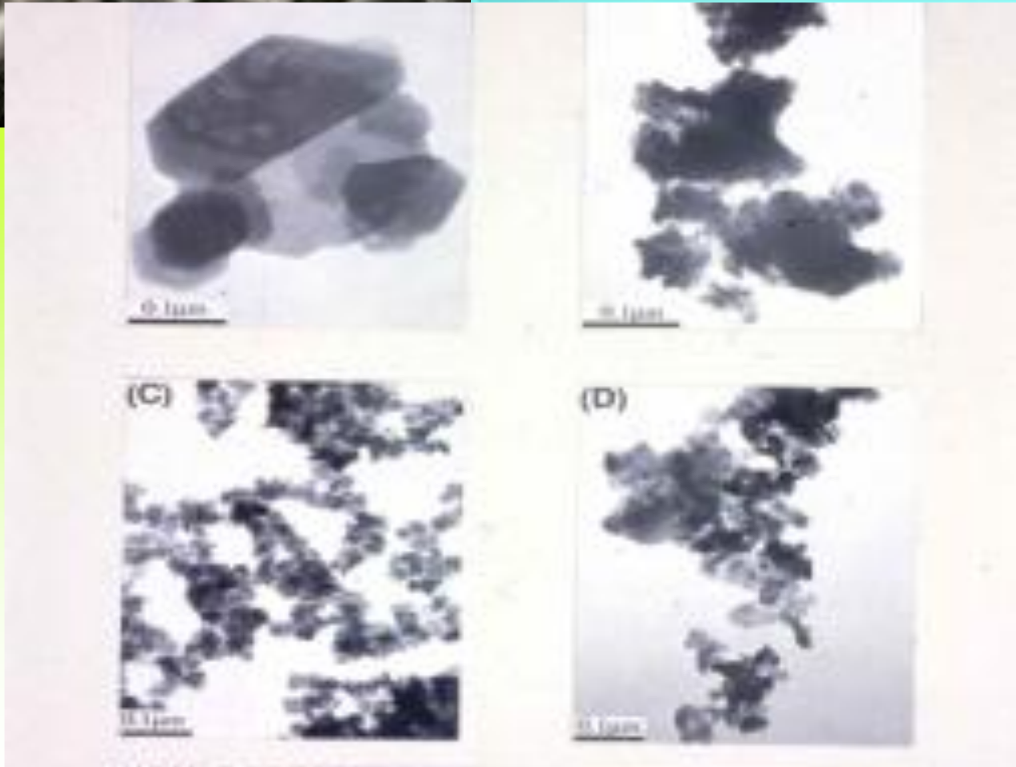

HIGH RESOLUTION TEM MICROGRAPHS OF

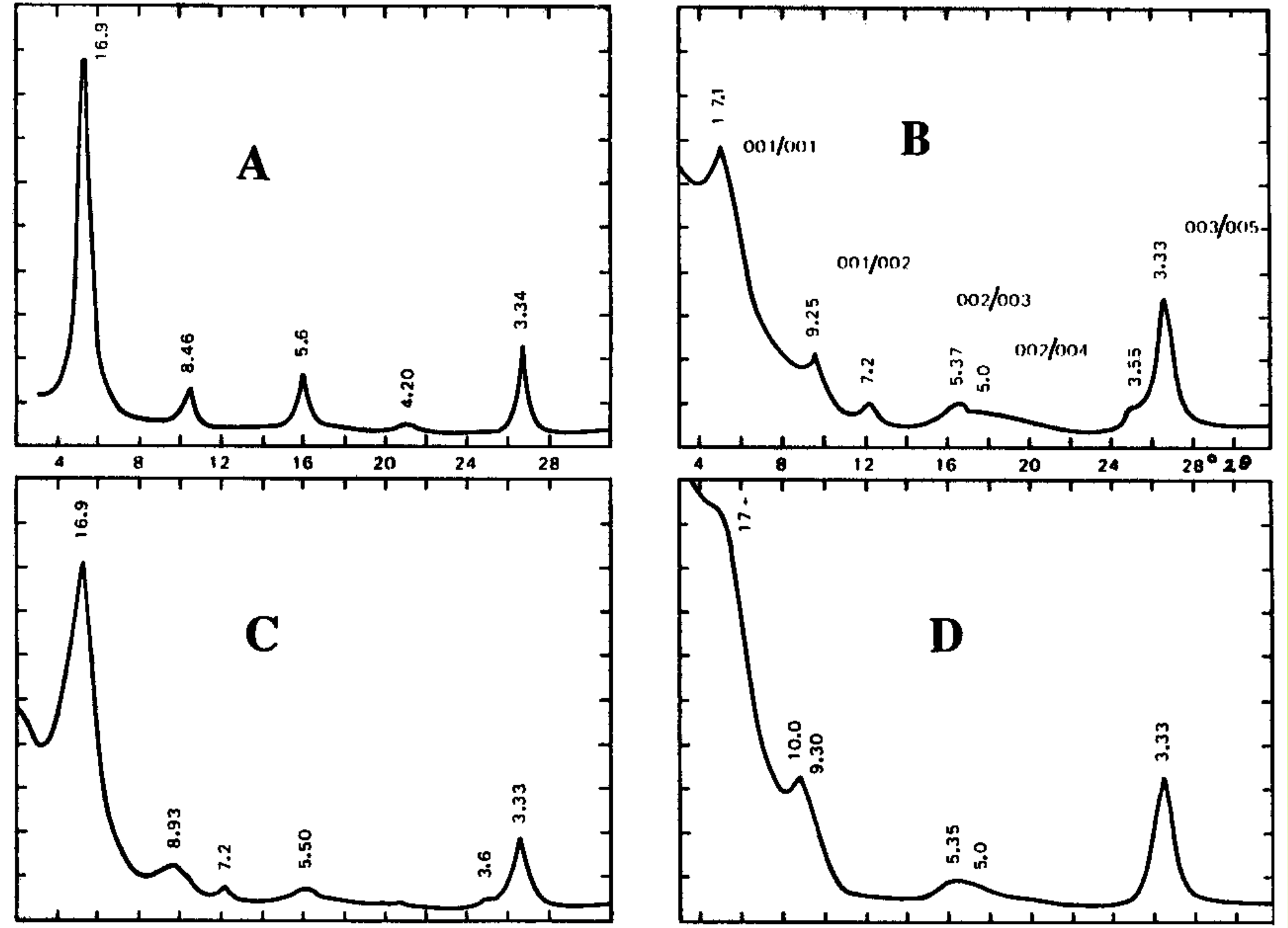

Diffraction patterns of ethylene glycol treated samples of montmorillonite, and randomly interstratified illite/montmorillonite. Percentages of montmorillonite layers: A, 100; B, 70; C, 50; and D, 40 (Reynolds and Hower, 1970).

Gibbsite

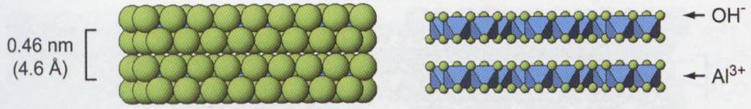

Kaolinite

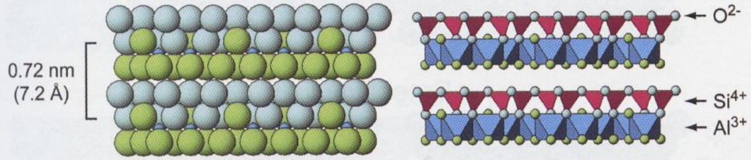

Halloysite (hydrated)

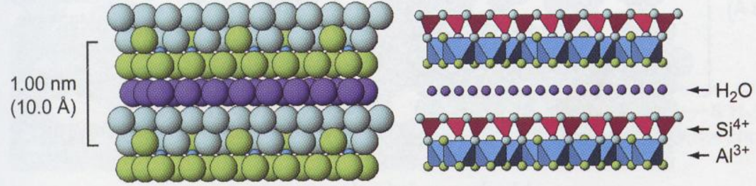

Pyrophyllite

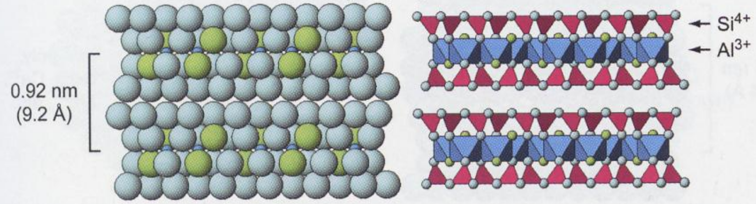

Mica (muscovite)

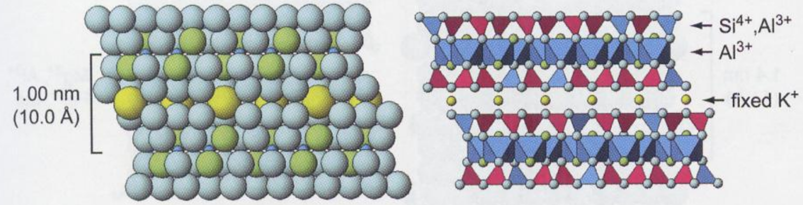

late 1–7. Structural scheme of soil minerals based on octahedral and tetrahedral sheets.

Table 12–1. Mineral species and formulas for some common 1:1 phyllosilicate species. More common examples are highlighted in bold fonts.

Species	Ideal formula†	Observed formula‡
Kaolin subgroup		
Kaolinite	$Al_2Si_2O_5(OH)_4$	$Al_2Si_2O_5(OH)_4$
Dickite	$Al_2Si_2O_5(OH)_4$	$Al_2Si_2O_5(OH)_4$
Nacrite	$Al_2Si_2O_5(OH)_4$	$Al_2Si_2O_5(OH)_4$
Halloysite (7Å)	$Al_2Si_2O_5(OH)_4$	$Al_2Si_2O_5(OH)_4$
Halloysite (10Å)	$Al_2Si_2O_5(OH)_4 \cdot 2H_2O$	$Al_2Si_2O_5(OH)_4 \cdot 2H_2O$
Serpentine subgroup (unmodulated members)		
Chrysotile	$Mg_3Si_2O_5(OH)_4$	$(Mg_{2.93}Fe^{3+}{}_{0.04}Fe^{2+}{}_{0.05})$ $(Si_{1.95}Al_{0.05})O_5(OH)_4$
Lizardite	$[Mg_{2.8}Al_{0.2}](Si_{1.8}Al_{0.2})O_5(OH)_4$	$(Mg_{2.12}Al_{0.88})(Si_{1.12}Al_{0.88})O_5(OH)_4$
Amesite	$[(Mg,Fe^{2+})_2Al](SiAl)O_5(OH)_4$	$[(Mg_{1.60}Fe^{2+}{}_{0.4})Al](SiAl)O_5(OH)_4$
Berthierine	$[(Fe^{2+},Mn^{2+},Mg)_{2.55\text{-}x0.15x}$§ $(Fe^{3+},Al)_{0.3+x}](Si_{2\text{-}x}Al_x)O_5(OH)_4$	$(Mg_{0.23}Al_{0.84}Fe^{3+}{}_{0.01}Fe^{2+}{}_{1.84})$ $(Si_{1.32}Al_{0.68})O_5(OH)_4$
Odinite	$[(Fe^{2+},Mn^{2+},Mg)_{2.5\text{-}x}$ $(Fe^{3+},Al)_x](Si,Al)_2O_5(OH)_4$	$(Mg_{0.77}Fe^{2+}{}_{0.28}Mn_{0.15}Fe^{3+}{}_{0.78}Al_{0.56}Ti_{0.02})$ $(Si_{1.79}Al_{0.21})O_5(OH)_4$
Serpentine subgroup (modulated members)		
Antigorite	$m[Mg_{3(1\text{-}1/m)}Si_2O_5(OH)_{1+3(1\text{-}2/m)}]$	$(Mg_{2.77}Al_{0.07}Fe^{3+}{}_{0.03}Fe^{2+}{}_{0.10})Si_2O_5(OH)_4$
Carlosturanite	$(Mg,Fe^{2+},Mn,Ti,Cr)_{21}$ $[(Si,Al)_{12}O_{28}(OH)_4]$ $(OH)_{30} \cdot H_2O$	$(Mg_{18.89}Fe^{2+}{}_{1.08}Ti_{0.55}Mn_{0.18}Cr^{3+}{}_{0.06})$ $[(Si_{11.46}Al_{0.41})O_{28}$ $(OH)_4](OH)_{30} \cdot H_2O$
Bementite	$Mn_5Si_4O_{10}(OH)_6$	

† Ideal formulas are from Bailey (1980, 1988), Brown (1984), and Guggenheim and Eggleton (1988).

‡ Observed formulas are from the JCPDS files (1983), Bailey (1988), Compagnoni et al. (1985), and Guggenheim and Eggleton (1988).

§ represents empty octahedral sites.

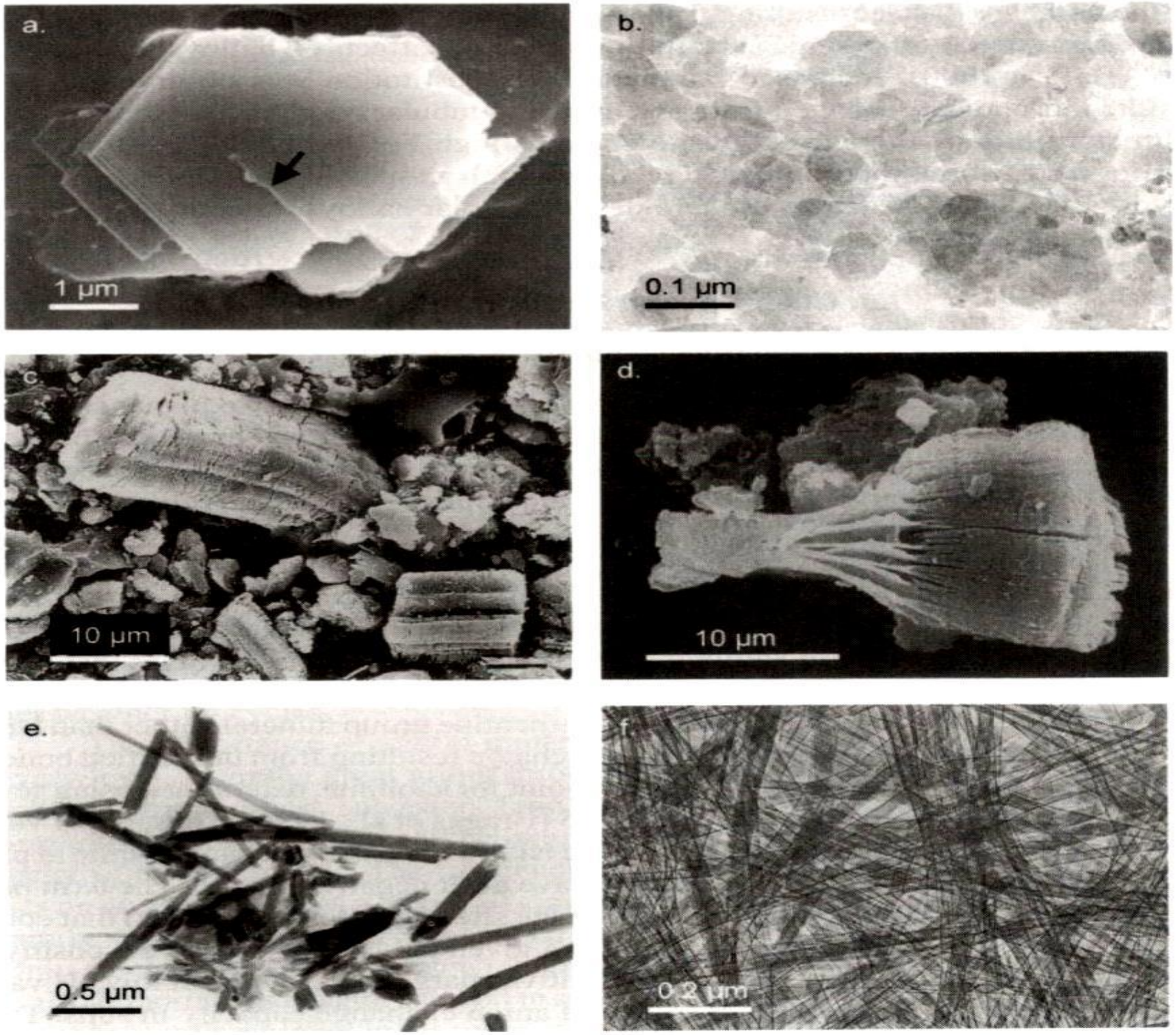

Fig. 12–1. Kaolinite and halloysite morphology. (a) Kaolinite from a Cretaceous limestone of Central Texas with a spiral growth step (arrow). (b) Thin, hexagonal kaolinite plates from a Katy Alfisol of southeast Texas. (c) Commercial grade kaolinite from Central Georgia composed of large vermiforms and smaller, complex aggregates. (d) Kaolinite vermiform (right) forming using muscovite (left) as a template from a Florida Spodosol (White & Dixon, 1997). (e) Tubular halloysite from saprolite beneath an Ultisol of the Alabama Piedmont. (f) An unusually uniform tubular halloysite from Australia with thin walls and fibers; aspect ratio 1:1200.

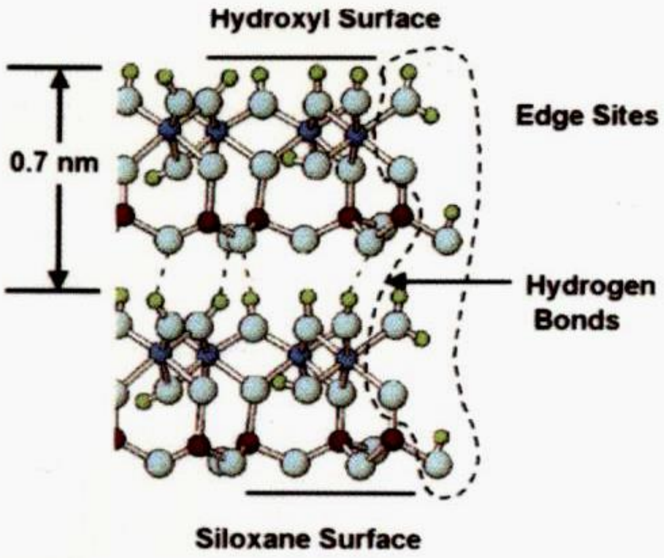

Plate 12–1. Structural diagram for kaolinite generated from the data of Young and Hewat (1988) with the edge sites predicted by White and Zelazny (1988).

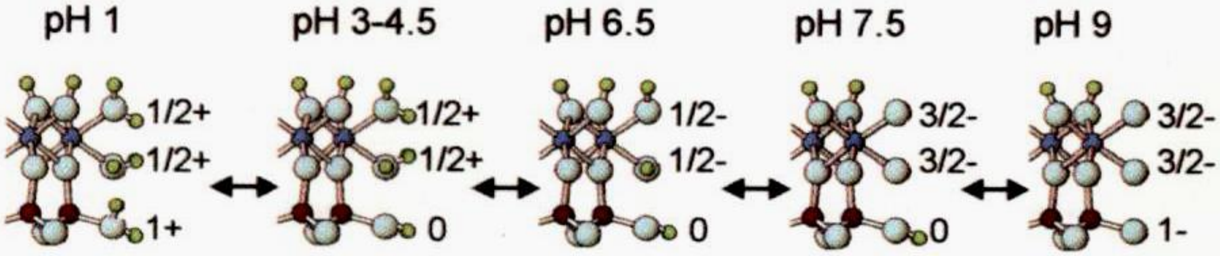

Plate 12–2. Effects of pH on the charge of the kaolinite edge that is affected by pH (modified from White and Zelazny, 1988). Color code for model is same as for Plates 12–1 and 12–3.

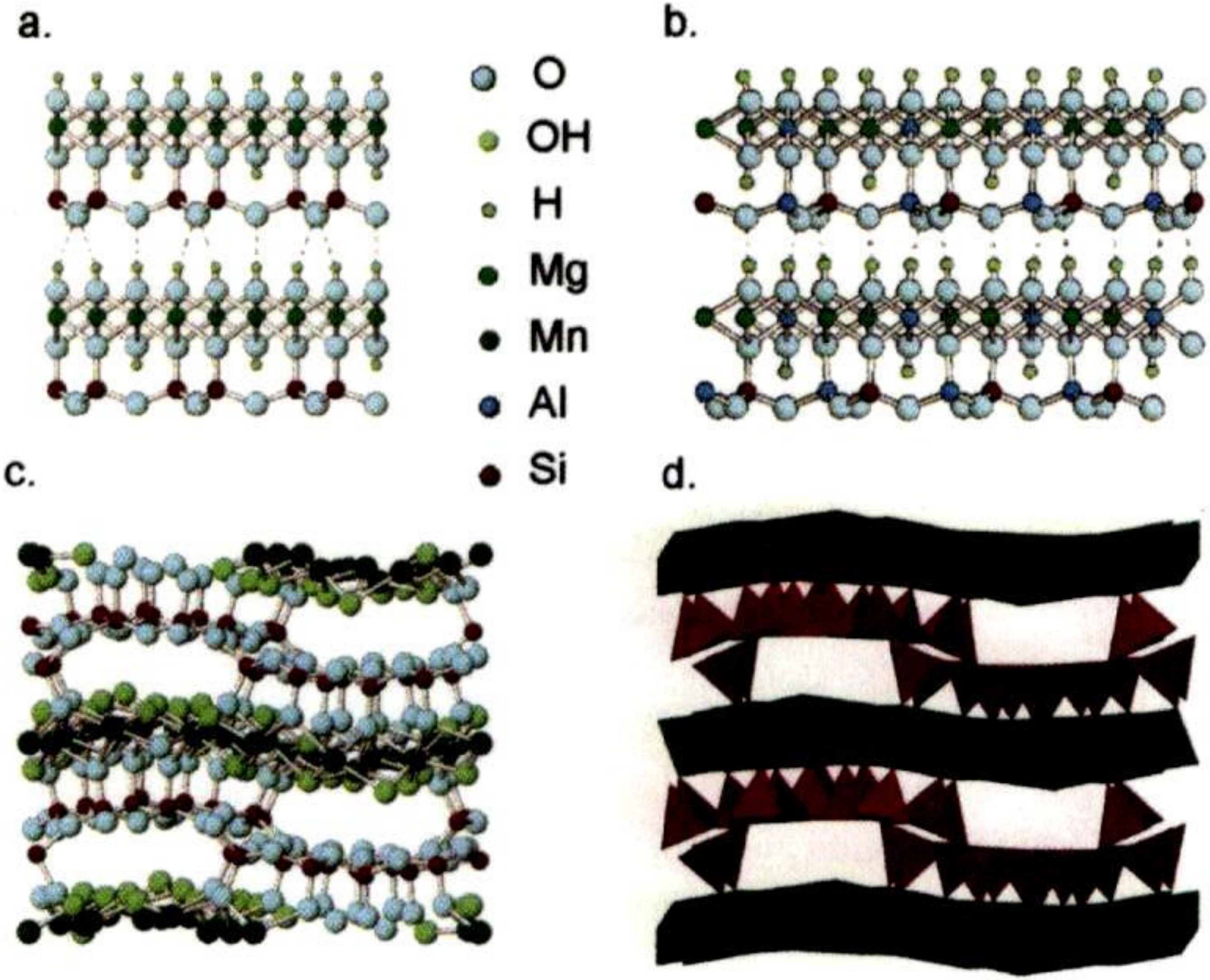

Plate 12–3. Calculated serpentine subgroup minerals structural schemes. (a) Lizardite - 1T from the data of Mellini and Viti (1994). (b) Amesite from the models of Hall and Bailey (1979) and Giese (1980). (c) Ball-and-stick model of the modulated trioctahedral 1:1 phyllosilicate, bementite, from the Heinrich et al. (1994) model. (d) Polyhedral model of bementite showing the wave pattern of the octahedral sheet.

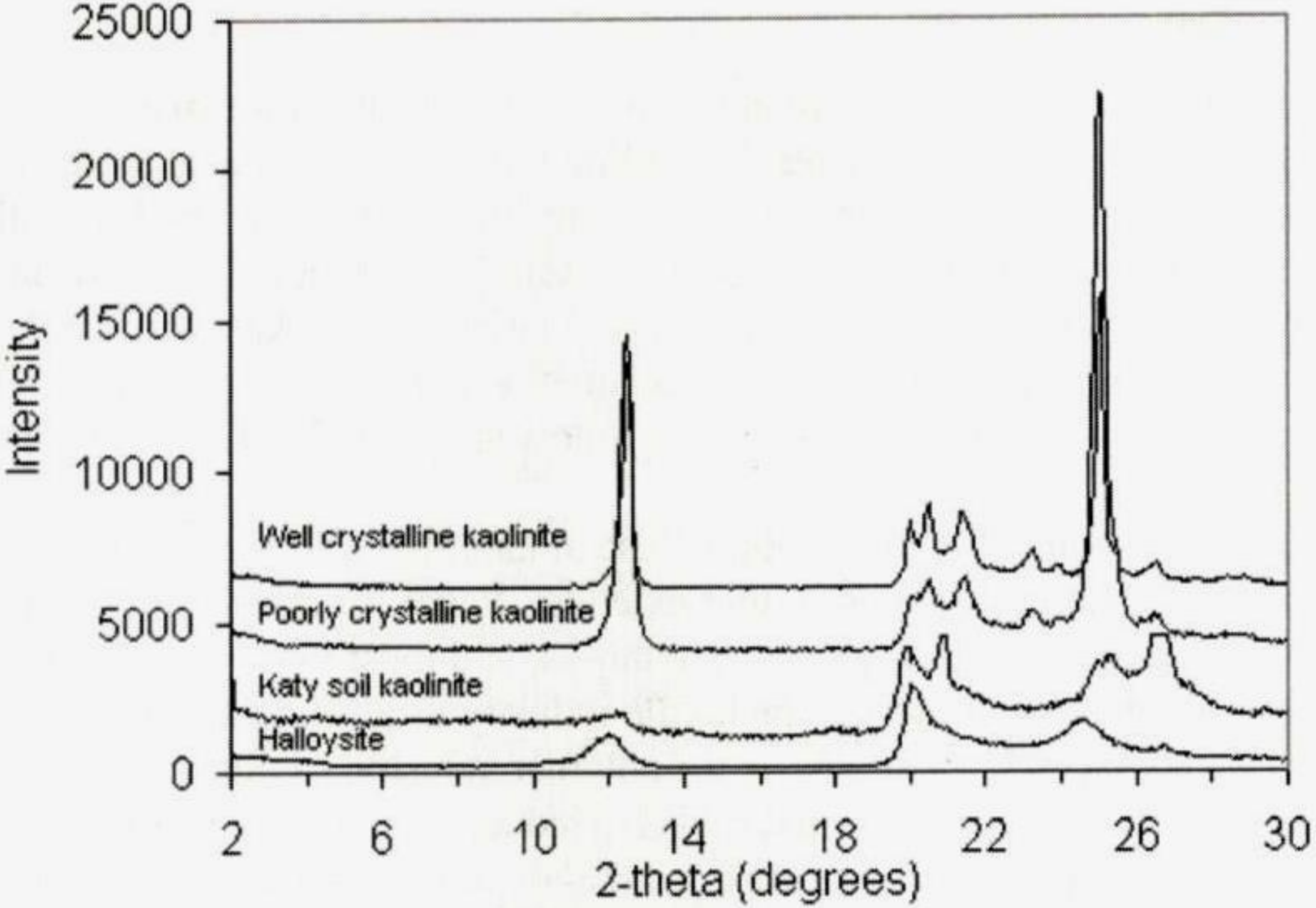

Fig. 12–2. X-ray powder diffraction curves for two specimen kaolinites, the kaolinitic clay from the Katy soil (Fig. 12–1b), and halloysite showing the range in expression of the prismatic peaks in the 0.45- to 0.35-nm region. The two truncated peaks on the soil kaolinite pattern represent quartz.

3. Morphology

Serpentines occur in three principal forms: platy, lath-like, and fibrous (Sudo et al., 1981). The edges are either irregular or bound by an apparent cleavage plane. Plates and laths are the principal morphologies for all members of the sub-

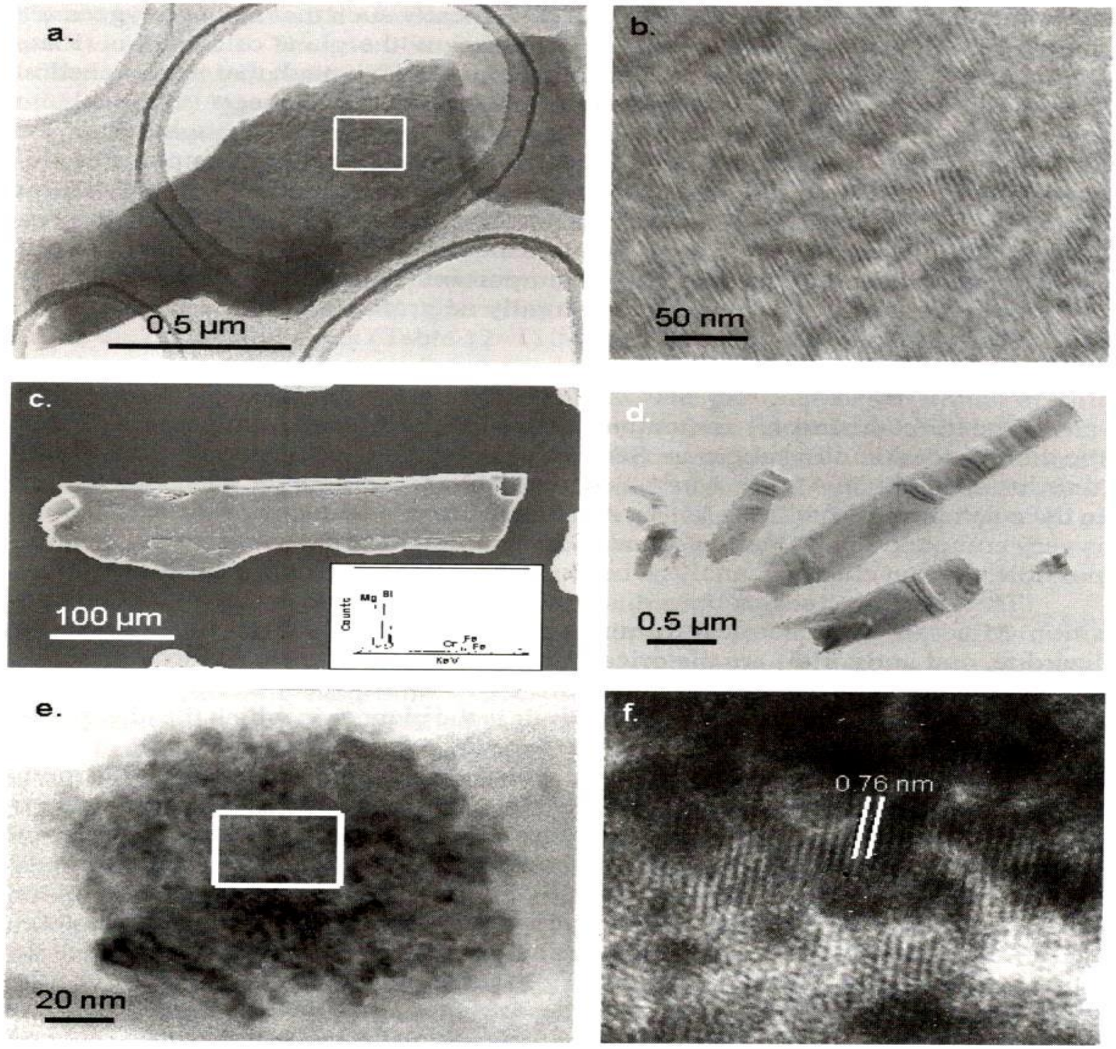

Fig. 12–3. Morphologies of serpentine subgroup minerals. (a) Modulated serpentine group mineral from the coarse clay fraction of a Honduran Inceptisol. (b) Higher magnification view of a portion of the modulated mineral grain outlined by the square in (a) showing the lattice fringes measuring 3.8 nm. (c) Serpentine lath containing Mg, Fe, and Cr from the Nipe Oxisol from Puerto Rico (White & Dixon, 1997). (d) Antigorite laths with characteristic rectangular terminations. (Source: Antigorio Valley, Italy; USNM # R-4648 provided by S. Guggenheim, Chicago, IL). (e) Serpentine occluded by Fe oxides from the Nipe soil clay. (f) Higher magnification view of the area of the particle in (e) outlined by the rectangle showing lattice fringes of serpentine.

HALLOYSITE

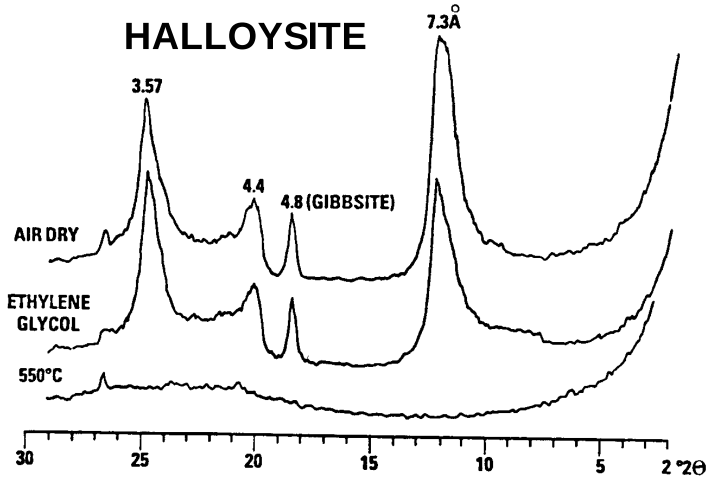

KAOLINITE

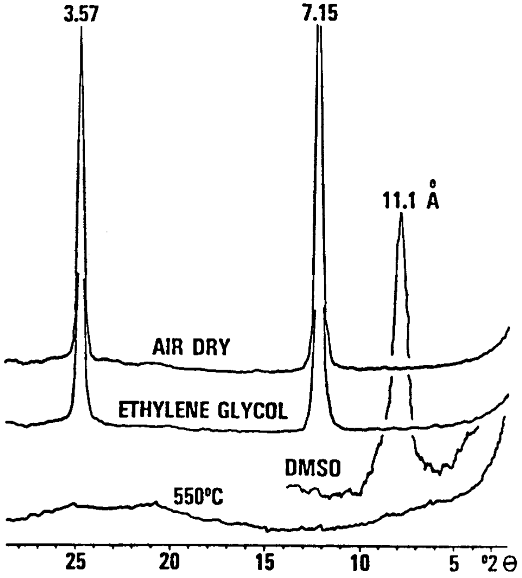

SERPENTINE

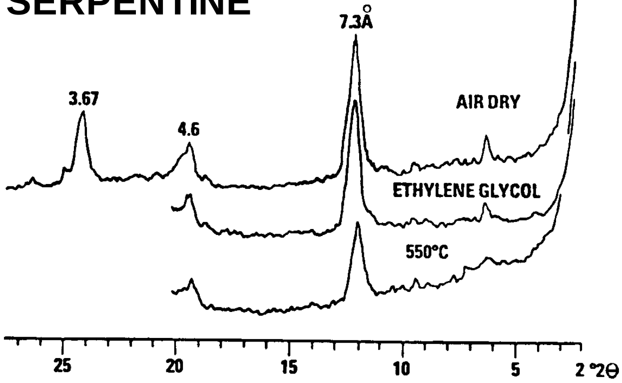

TALC

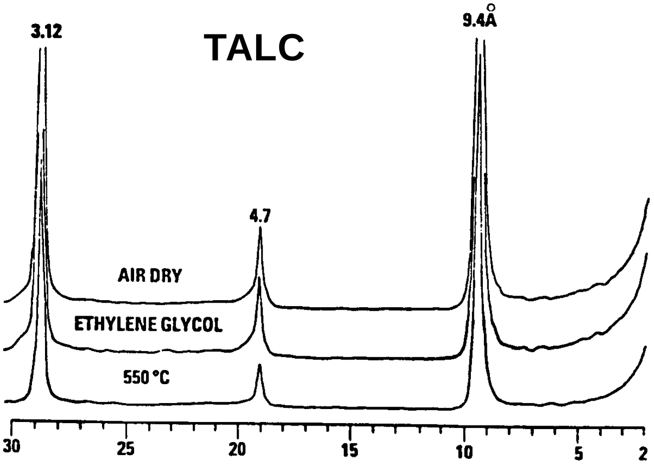

ILLITE

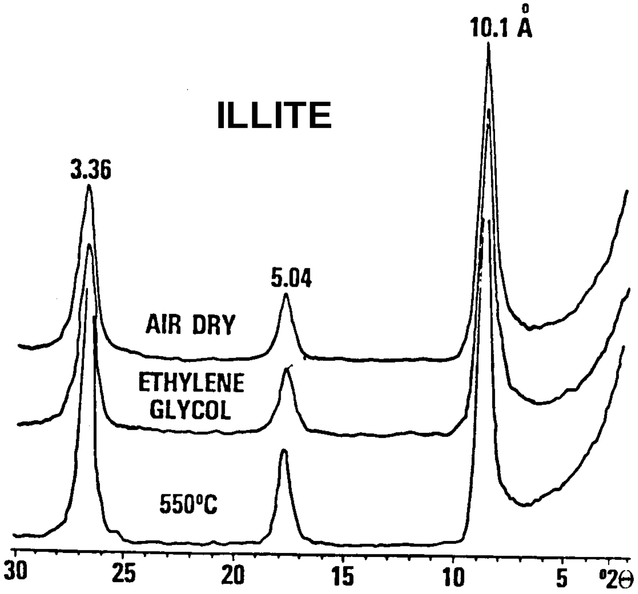

VERIMICULITE

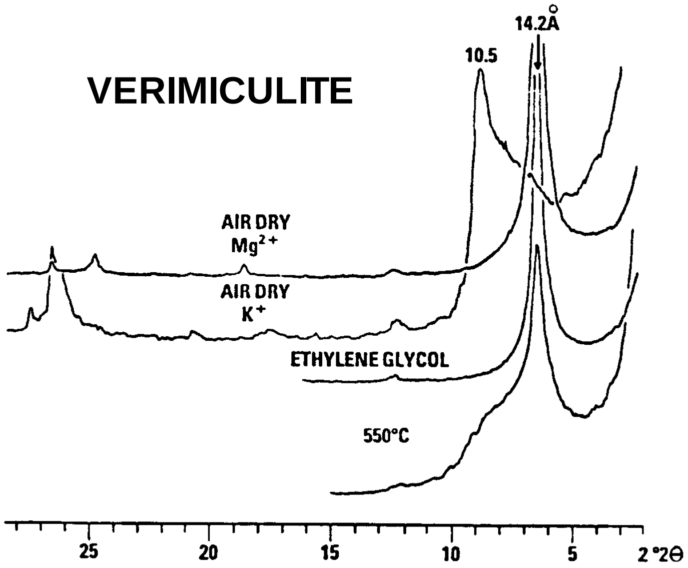

SMECTITE

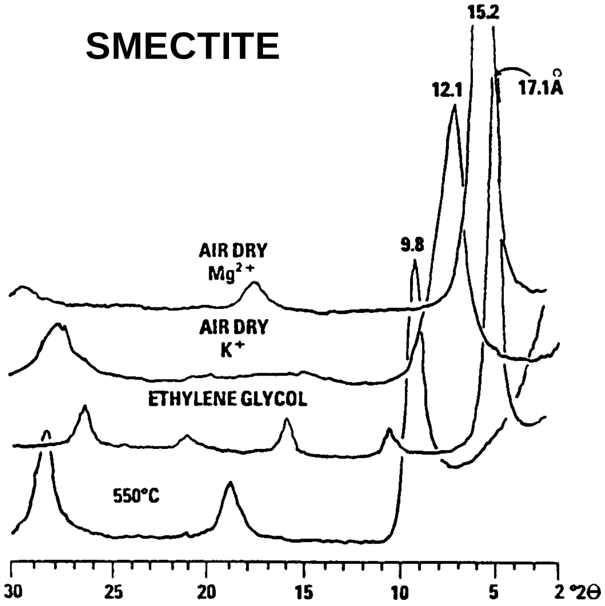

CHLORITE

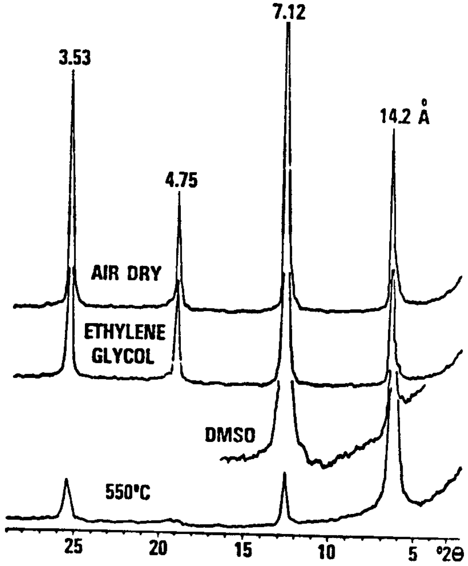

Table 13–1. Theoretical and representative observed formulas for members of the pyrophyllite–talc group.

	Ideal formula				Representative observed formula‡			
Mineral and reference†	Interlayer	Octahedral	Tetrahedral	Anions	Interlayer	Octahedral	Tetrahedral	Anions
					Dioctahedral			
Pyrophyllite (1)	--	Al_2	Si_4	$O_{10}(OH)_2$	$M^{+}_{0.01}$§	$Al_{2.01}Fe^{2+}_{0.01}Mg_{0.02}$	$Si_{3.88}Al_{0.12}$	$O_{10}(OH)_2$
Ferripyrophyllite (2)	--	Fe^{3+}_2	Si^4	$O_{10}(OH)_2$	$M^{+}_{0.10}$	$Fe^{3+}_{1.87}Mg_{0.11}Al_{0.09}$	$Si_{3.80}Fe^{3+}_{0.16}Al_{0.04}$	$O_{10}(OH)_2$
					Trioctahedral			
Talc (1)	--	Mg_3	Si_4	$O_{10}(OH)_2$	$M^{+}_{0.02}$	$Mg_{2.89}M^{3+}_{0.03}M^{2+}_{0.10}$	$Si_{3.97}Al_{0.03}$	$O_{10}(OH)_2$
Willemseite (3)	--	Ni_3	Si_4	$O_{10}(OH)_2$	$M^{+}_{0.04}$	$Ni_{2.11}M^{2+}_{0.80}M^{3+}_{0.10}$	$Si_{3.93}Al_{0.07}$	$O_{10}(OH)_2$
Minnesotaite (3)¶	--	Fe^{2+}_3	Si_4	$O_{10}(OH)_2$	$M^{+}_{0.01}$	$Fe^{2+}_{2.16}M^{2+}_{0.71}M^{3+}_{0.12}$	$Si_{3.93}Al_{0.07}$	$O_{10}(OH)_2$
Kerolite (4)	xH$_2$O#	Mg_3	Si_4	$O_{10}(OH)_2$	$M^{+}_{0.04}\bullet xH_2O$	$Mg_{2.98}M^{2+}_{0.02}$	$Si_{3.96}Al_{0.04}$	$O_{10}(OH)_2$
Pimelite (4)	xH_2O	Ni_3	Si_4	$O_{10}(OH)_2$	xH_2O	$Ni_{2.90}M^{2+}_{0.10}$	Si_4	$O_{10}(OH)_2$

† References for observed formulas: (1) Koster (1982), (2) Coey et al. (1984), (3) De Waal (1970), and (4) derived from observed formulas in Brindley et al. (1979).

‡ Discrepancy in 22 charge basis of observed formulas for pyrophyllite, talc, willemseite, and minnesotaite maybe due to rounding errors or presence of impurities.

§ M = metal cation of valency given.

¶ Minnesotaite is included here but may be placed more appropriately with modulated layer structures (Martin et al., 1991).

Location of H_2O in all kerolite and pimelite structures is likely on external surfaces as well as within interlayer. x = value ranging from 0.8 to 1.2 (Brindley et al., 1979).

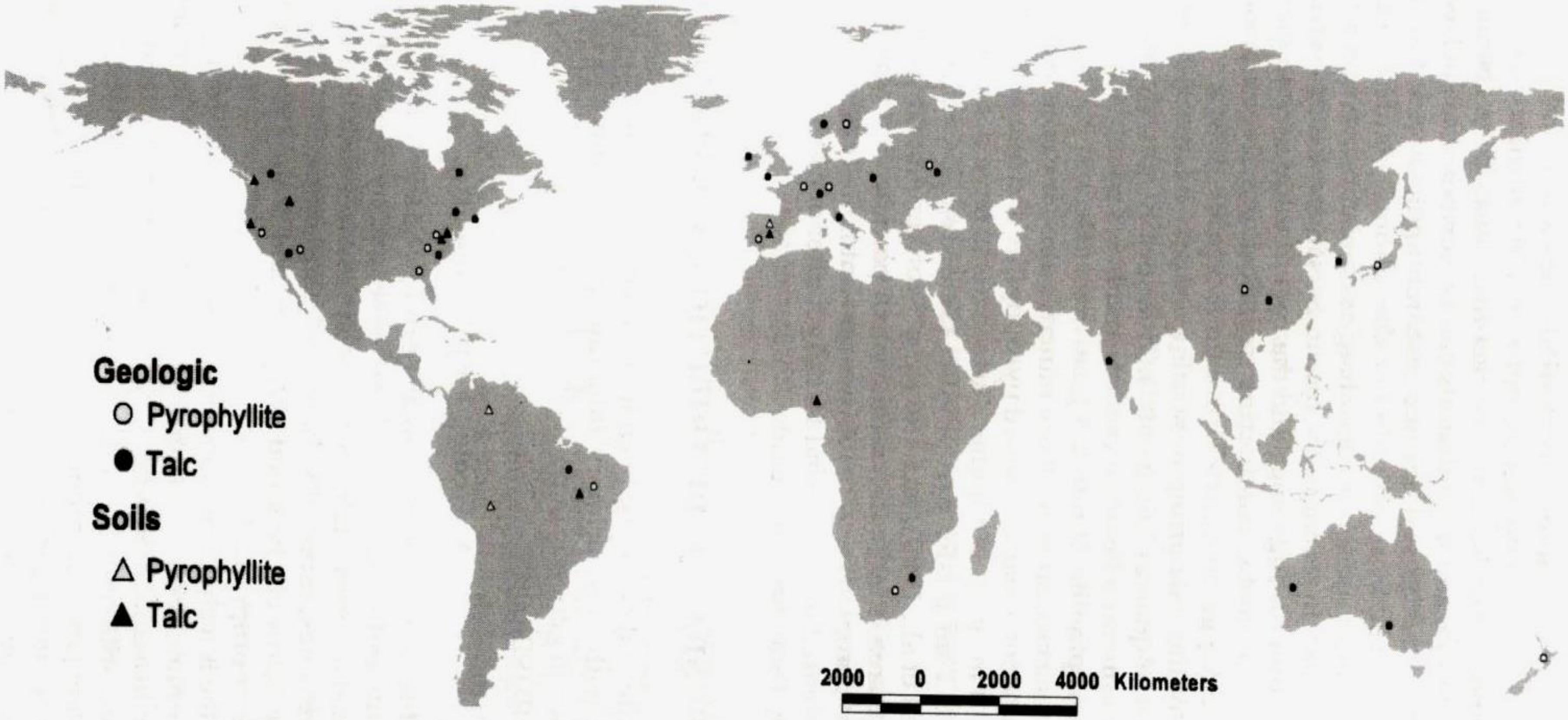

Fig. 13–1. Worldwide distribution of reported pyrophyllite and talc in geologic and soil settings.

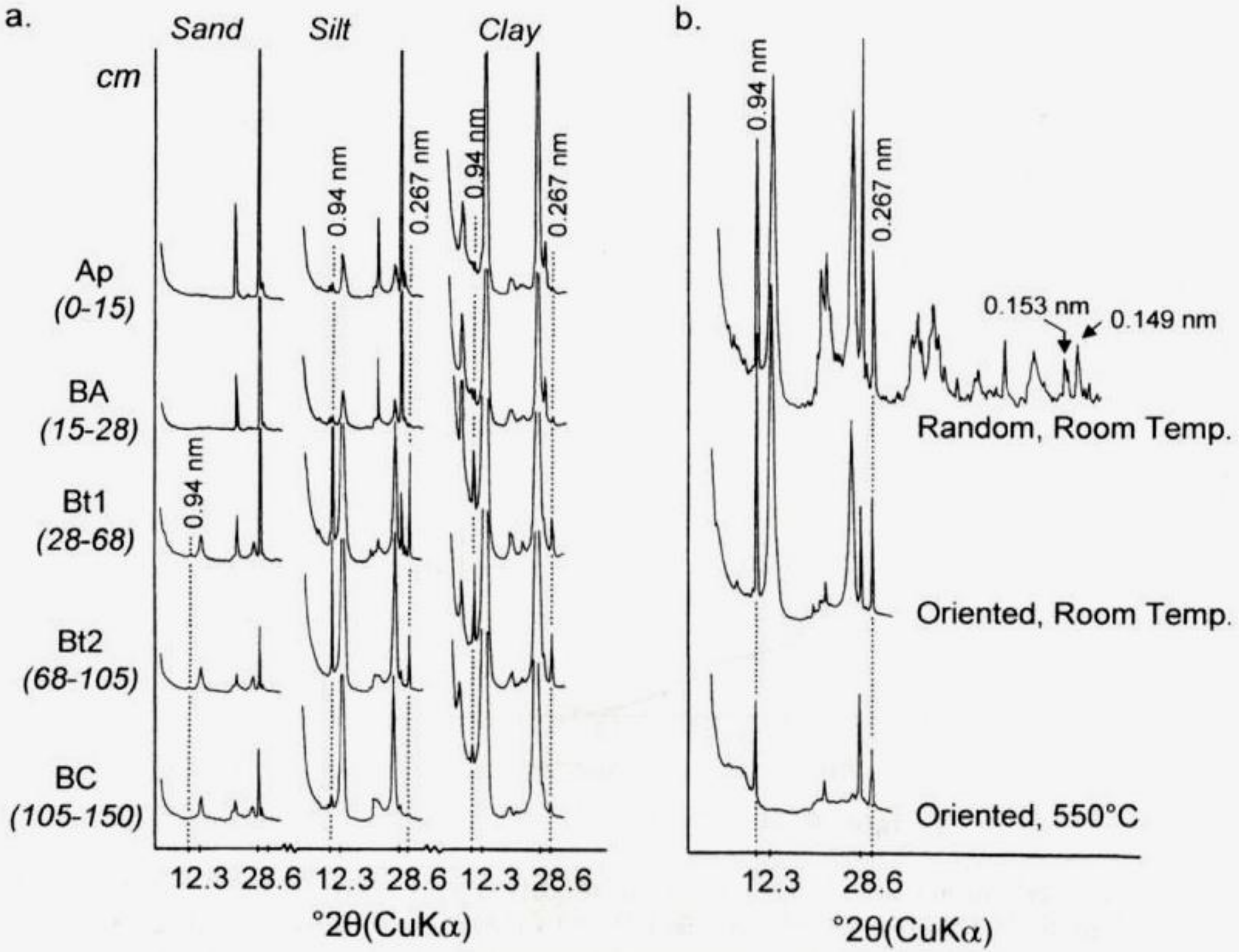

Fig. 13–2. X-ray powder diffraction patterns (modified from Harris et al., 1984): (a) for oriented mounts of clay, silt, and ground sand fractions from different depths of a Virginia Piedmont Ultisol. Talc is identified by peaks at 0.94 (001) and 0.267 (003) nm; (b) for the Bt1 silt fraction of a random and oriented mount at room temperature and for an oriented mount after heating to 550°C for 9 h. In a random mount, talc can also be identified by the 0.153- (060) nm peak. Also observe that the 0.94- and 0.267-nm peaks for talc are stable after heating to 550°C, whereas kaolinite (0.72 nm) is destroyed.

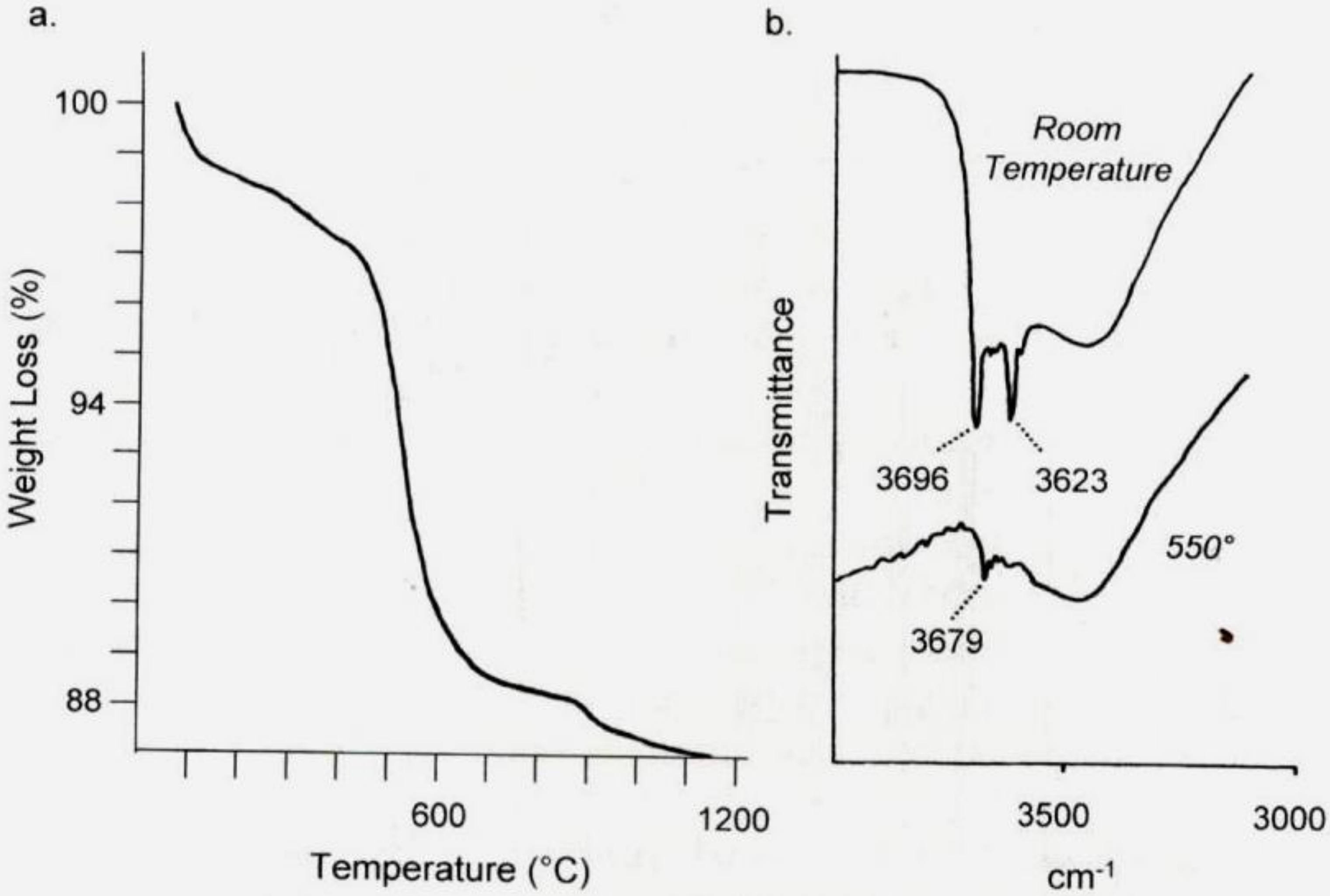

Fig. 13–3. Characterization of the Bt1 silt fraction (modified from Harris et al., 1984) by: (a) Thermal gravimetric analysis. Observe weight loss from 840 to 1000°C, which is equivalent to 14% talc. The large weight loss from 400 to 700°C is equivalent to 56% kaolinite. (b) Infrared analysis at room temperature and after heating to 550°C for 9 h. Observe talc peak at 3679 cm^{-1}, which is small at room temperature, but persists after heating to 550°C. The kaolinite peaks at 3696 and 3623 cm^{-1} are large at room temperature but are lost after heating to 550°C.

Criteria for Classification

1. *Type of tetrahedra octahedra sheet combination,*
2. *Types and amounts of cations in octehedral sheets dioktahedral, trioktahedral,*
3. *Layer Charge,*
4. *Type of interlayer cations,*
5. *Overall chemical composition,*
6. *Polytypes (layer stacking) and nature of stacking.*

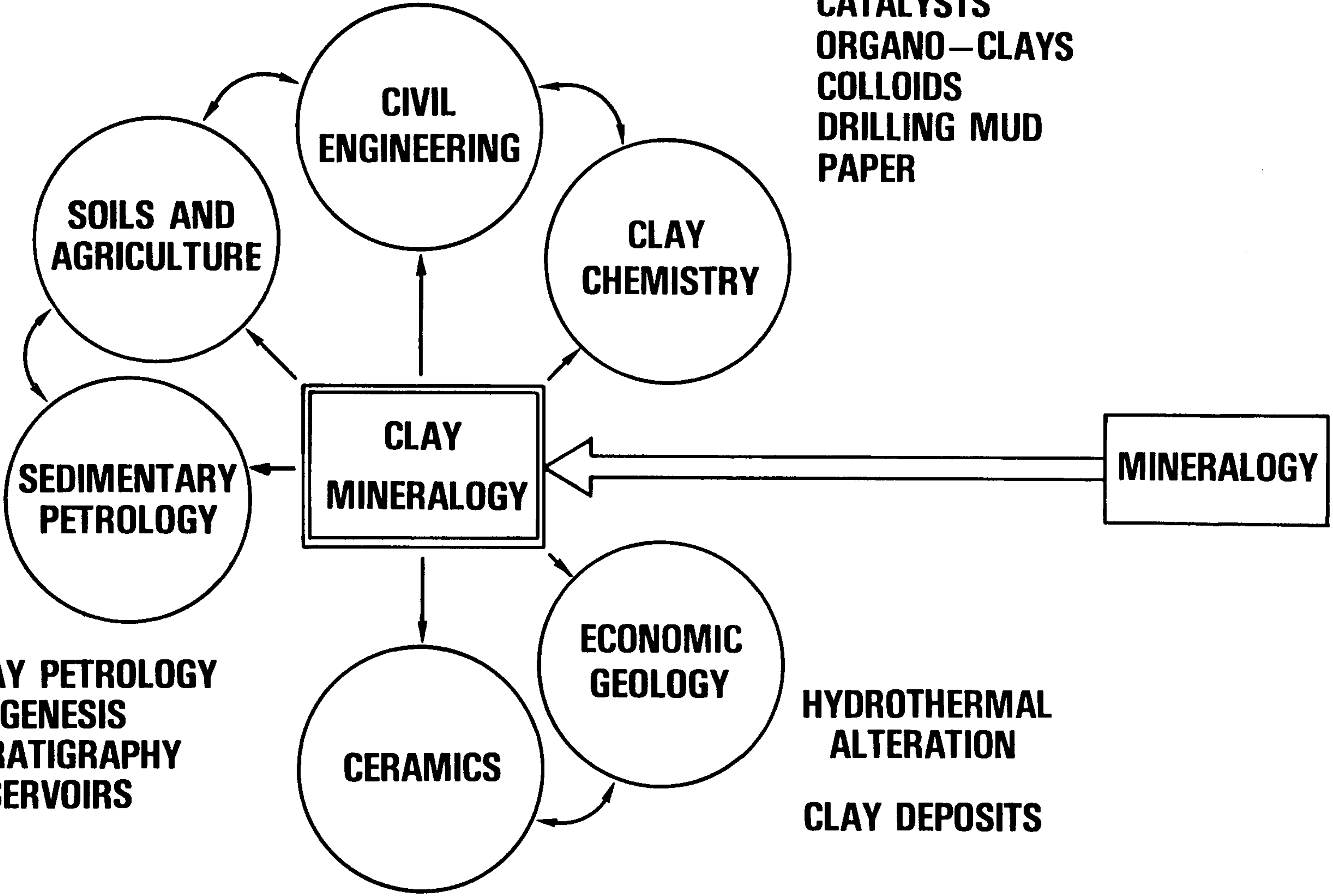

CLAY MINERALOGY

MINERALOGY

CIVIL ENGINEERING

SOILS AND AGRICULTURE

CLAY CHEMISTRY

SEDIMENTARY PETROLOGY

CERAMICS

ECONOMIC GEOLOGY

CATALYSTS
ORGANO—CLAYS
COLLOIDS
DRILLING MUD
PAPER

CLAY PETROLOGY
DIAGENESIS
STRATIGRAPHY
RESERVOIRS

HYDROTHERMAL ALTERATION

CLAY DEPOSITS

Origin and Distribution

- **They are found in the outer layer of of earth,**
- **Results of the mineral alteration with hydrosphere,**
- **Occurs in < 500ºC environment,**
- **Soils, sedimentary rocks are the most abundant, shales is the most common**

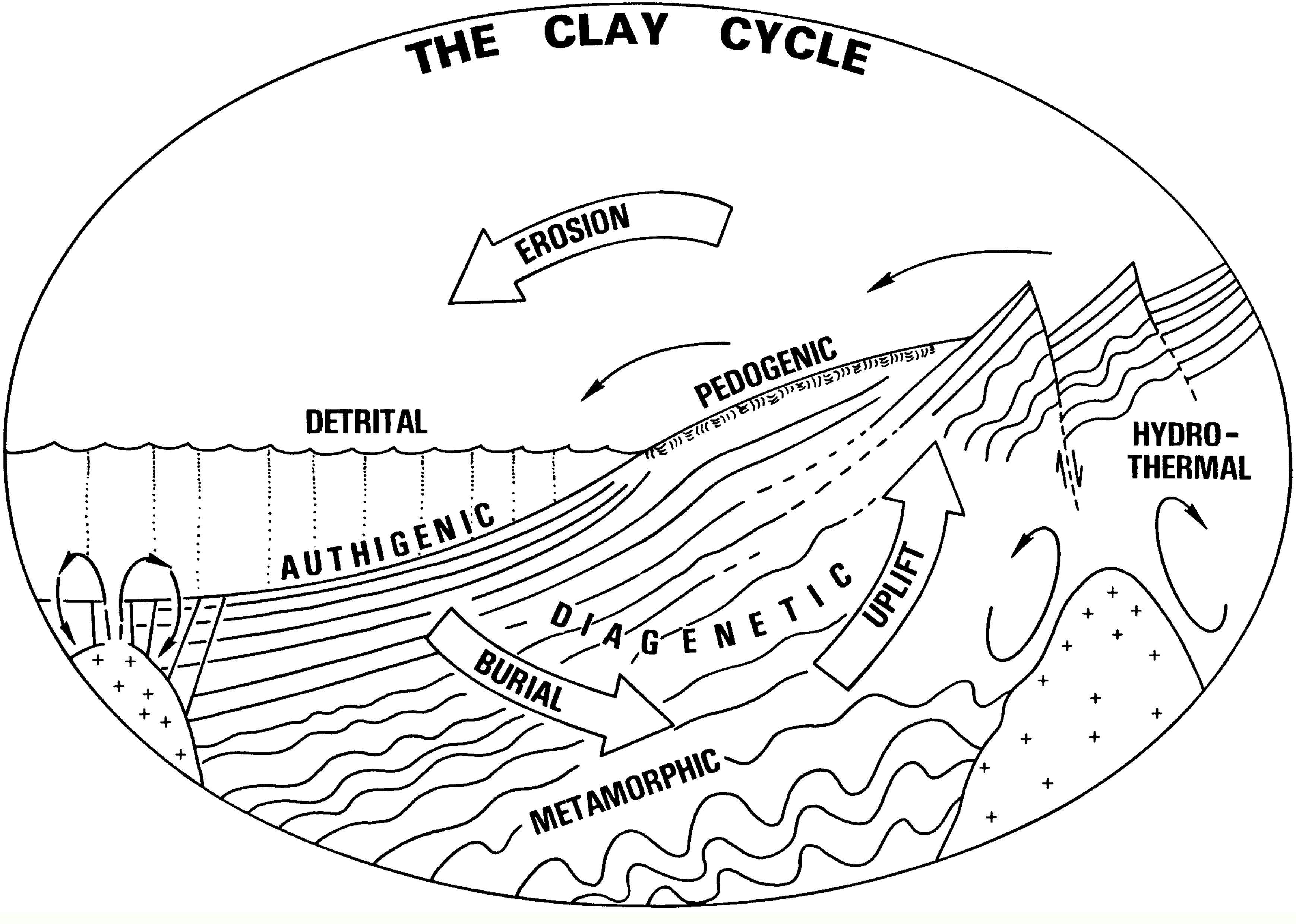
THE CLAY CYCLE
EROSION
PEDOGENIC
DETRITAL
AUTHIGENIC
DIAGENETIC
BURIAL
UPLIFT
HYDRO-
THERMAL
METAMORPHIC

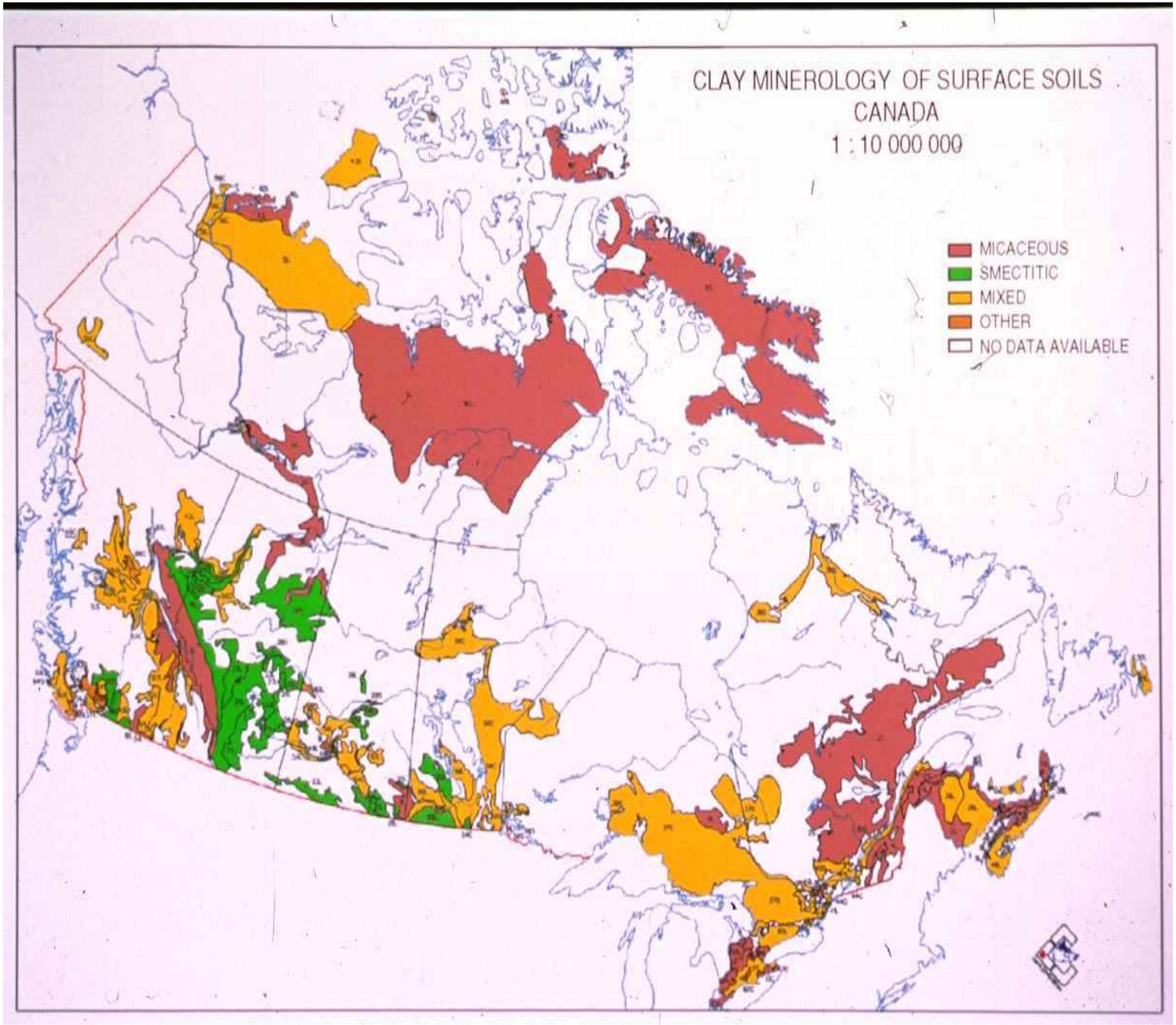

Mermut, A. R and H. Kodama. 1999. Clay Mineralogy of Canadian soils. Proceed. 11th International Clay conference, Ottawa. Published ICC 97 Org. Com.